

**On the exposure assessment  
of engineered nanoparticles  
in aquatic environments**

---



# On the exposure assessment of engineered nanoparticles in aquatic environments

---

**Julián Alberto Gallego Urrea**



GÖTEBORGS UNIVERSITET

Akademisk avhandling för filosofie doktorsexamen i naturvetenskap  
med inriktning kemi, som med tillstånd från Naturvetenskapliga  
fakulteten kommer att offentligt försvaras fredagen den 17 januari, 2014,  
kl. 10:15 i KB, Institutionen för kemi och molekylärbiologi, Kemigården  
4, Göteborg.

Institutionen för kemi och molekylärbiologi

Naturvetenskapliga fakulteten

Göteborgs Universitet

ISBN: 978-91-628-8874-9

e-ISBN: 978-91-628-8875-6

On the exposure assessment of engineered nanoparticles in aquatic environments

JULIÁN ALBERTO GALLEGO URREA, 2013.

ISBN 978-91-628-8874-9

Electronic version ISBN 978-91-628-8875-6

Available on-line:

<http://hdl.handle.net/2077/34386>

Cover picture: Photography and drawing of the sedimentation experiments with NOM, ENP, NNP and IS (photo: Julia Hammes; see content for abbreviations). Map of European watersheds colored according to Debye length (red larger than green). Results from NTA measurements after 2 months experiments of Au NP and illite in microcosms with MNW I (up) and VI (down) (from Paper VI).

Printed by:

Ale Tryckteam, Bohus 2013

A Maria y a mis padres

Por su persistente apoyo

FP



## **Abstract**

The socio-economic benefits anticipated with the use and production of nanomaterial and nanoparticles in consumer products are linked to the fulfillment of the requirement for sustainability during the whole material life cycle. Engineered nanoparticles (ENP) can be of environmental concern, both due to the possible hazardous effects but also due to the differences in properties compared to regular chemicals, e.g. elevated surface area per mass of nanoparticle, the possibility for enhanced mobility and trespassing biological membranes and other emerging novel properties at the nanoscale. There is a scientific consensus that nanoparticles, nanomaterials and their transformation products have a high probability to be released in the environment. ENP in the aquatic environment present a very dynamic behavior that has to be understood in order to perform a physicochemical-based risk assessment that elucidates their transformation and transport leading to the possibility to predict environmental concentrations and exposure. Therefore, there is a need for adequate theoretical and experimental platforms that can be used for supporting the adequate assessment of fate processes of ENP in the environment.

The structure of the thesis is aimed to remark the results obtained in the papers by first creating a theoretical background for fate processes of ENP in the environment that is later used to analyse the results obtained focusing on the specific processes studied in the papers, i.e. aggregation and agglomeration, heteroaggregation, shape effects on particle characterization and sedimentation. Alongside the theoretical sections some reference to the papers is done when the relevance of the specific subject is adequate. Some definite examples in the theoretical sections are related to the experimental part as well. Chapter 1 gives a background about nanotechnology and ENP and introduces the concepts involved in risk assessment of chemicals and how these can be applied to the case of ENP making emphasis on the fate processes; it also explains the complexity involved in the exposure assessment of ENP, e.g. the dynamicity of the systems and the interactions with natural constituents of the receiving water bodies. Chapter 2 gives a brief description of particle characteristics that can affect the fate processes including the definitions of the different equivalent spherical diameters for different shapes, number concentrations, surface charge and particle

coating. Chapter 3 gives the basic theoretical framework and some state of the art information that can be relevant to understand the different processes that can affect ENP transport and transformation in the environment. Chapter 4 is dedicated exclusively to describe the geographical classification of European water chemistry as a platform for evaluating the different fate processes of ENP in environment. Chapter 5 describes the different findings from the papers related to environmental fate processes of ENP like aggregation, natural organic matter (NOM) coating, heteroaggregation and sedimentation.

The main results achieved in the thesis were reflected in: 1) identification of theoretical platforms that can provide solutions for the evaluation of fate processes of ENP in aquatic environments 2) improvement in the application of a novel particle tracking method for characterizing natural nanoparticles and ENP in different matrices; 3) identification of the effects of well-characterized NOM and counterion valence on the aggregation rates of TiO<sub>2</sub> nanoparticles 4) developing a geographically distributed water classification for Europe based on river water chemistry, 5) use the geographical water classification to evaluate the aggregation and sedimentation of Au NP in in-situ quiescent-water microcosms.

The physicochemical characteristics of the receiving water were found to be very influential on the fate of the ENP tested. The ionic concentration, presence of divalent counter ions (specifically calcium), the type of NOM and mass-ratio between NOM and the particles are among the most important parameters. NP coating, surface charge, material properties and shape will also play very important roles. NP number concentrations determine the degree of transport and transformation due to the different dynamic processes in the environment.



## Populärvetenskaplig sammanfattning

Det finns ett antal krav från samhället som behöver tekniska utvecklingar som kan hjälpa till att lösa dem. Bland de senaste teknikerna som har utvecklats finns nanoteknik som är en av de tekniker som har fått uppmärksamhet. Nanoteknik är inte nytt i sig, men under det senaste århundradet har den vuxit fram som ett resultat av en kontinuerlig uppdatering av analysen av mikroskala processer. Nanoteknologi handlar om manipulering av objekt på nanometerskala (d.v.s. under 100 nm).

Nanopartiklarna är en del av det som nanotekniken har att erbjuda. De består av små obundna partiklar med storlek under 100 nm. Dock är nanoteknik inte den enda källan till nanopartiklar för miljön; det finns naturliga partiklar som resultat av geologiska, kemiska och biologiska processer. Till exempel lermineral som kommer från bergartserosion, organiska ämnen som kommer från utsöndringar av växter och djur, nedbrytning av biologiskt material eller fällning från vissa kemikalier som kan forma små kristaller i nanometerskala. Därför är identifiering av tillverkade nanopartiklar i miljön en utmaning eftersom de måste skiljas från de naturliga nanopartiklarna.

För att utveckla och använda nanomaterial på ett ansvarfullt sätt är det av största vikt att kunna göra uppskattningar av exponeringssituationen för riskbedömningar. Avhandlingen består av en teoretisk sammanfattning som grund för att utveckla modeller och experimentella inställningar som kan hjälpa till att belysa utsläppen, nanoföremålens slutliga öde, omvandling och möjliga vägar av exponering. Ett set av sex Europeiska naturliga vatten med gemensamma kemiska egenskaper identifierades med hjälp av statistiska- och geografiska verktyg. Vattenklasserna kan hjälpa att bedöma omvandlings- och transportprocesser för nanopartiklarna i den Europeiska vattenmiljön. Ett experiment med de sex vattenklasser som inkluderade en typ av organiskt material och en lerminerall som är mycket vanliga i vattenmiljön gjordes för att utvärdera aggregering och sedimentering av små mängder guld nanopartiklarna. Guld nanopartiklarna var mycket stabila mot aggregering i fyra vattenklasser och mindre stabila i de vattenklasser som innehöll stora mängder av joner. Naturell organiskt material visade sig att vara betydelsefull för att avgöra ödet av

nanopartiklarna i vattenmiljö. Eftersom det finns många olika typer av naturell organiskt material då kan det inte avgöras att stabilisering kommer att vara universellt.

Studier med nanopartiklarna kan hjälpa att förbättra hur miljö-och hälsoriskbedömning har gjorts konventionellt till andra ämnen.

# Table of Contents

<b>1.</b>	<b>INTRODUCTION AND BACKGROUND.....</b>	<b>1</b>
1.1.	NANOTECHNOLOGY AND THE ENVIRONMENT .....	1
1.2.	WHAT ARE NANOMATERIALS AND NANOPARTICLES? .....	2
1.3.	ENVIRONMENTAL NANOSAFETY RESEARCH .....	4
1.4.	AIM AND APPROACH .....	8
<b>2.</b>	<b>NANOPARTICLE CHARACTERISTICS .....</b>	<b>11</b>
2.1.	NANOPARTICLE SIZE AND EQUIVALENT DIAMETER .....	11
2.2.	NANOPARTICLE SHAPE.....	11
2.3.	NUMBER CONCENTRATIONS AND PARTICLE SIZE DISTRIBUTION .....	15
2.4.	SURFACE CHARGE.....	17
2.5.	SURFACE COATING.....	20
<b>3.</b>	<b>THEORETICAL FRAMEWORK FOR PARTICLE FATE.....</b>	<b>21</b>
3.1.	BROWNIAN DIFFUSION .....	21
3.2.	COLLOIDAL STABILITY .....	24
3.3.	EFFECTS OF NOM ON COLLOIDAL STABILITY .....	28
3.4.	COLLISIONS BETWEEN PARTICLES.....	29
3.5.	SEDIMENTATION .....	33
3.6.	LARGE SCALE MODELS.....	36
<b>4.</b>	<b>ENP FATE PLATFORM ON A CONTINENTAL WATERSHED SCALE</b>	<b>38</b>
<b>5.</b>	<b>FATE PROCESSES .....</b>	<b>43</b>
5.1.	AGGREGATION AND AGGLOMERATION .....	44
5.2.	NOM-SORPTION: EFFECTS ON STABILITY.....	47
5.3.	SEDIMENTATION .....	48
<b>6.</b>	<b>CONCLUDING REMARKS AND FUTURE PERSPECTIVES.....</b>	<b>56</b>
<b>7.</b>	<b>ACKNOWLEDGEMENTS.....</b>	<b>60</b>
<b>8.</b>	<b>REFERENCES .....</b>	<b>62</b>

## List of Scientific Publications

This thesis is based on the following research articles and reference to them will be done using the roman numerals. The articles are appended at the end of the printed version of the thesis:

- Paper I. Gallego-Urrea, J. A.; Tuoriniemi, J.; Pallander, T.; Hassellöv, M. Measurements of nanoparticle number concentrations and size distributions in contrasting aquatic environments using nanoparticle tracking analysis. *Environmental Chemistry*. Vol. 7 (1) pp. 67-8. 2009
- Paper II. Gallego-Urrea, J. A.; Tuoriniemi, J.; Hassellöv, M. Applications of particle-tracking analysis to the determination of size distributions and concentrations of nanoparticles in environmental, biological and food samples. *Trac-Trends in Analytical Chemistry*. Vol. 30 (3) pp. 473-483. 2011
- Paper III. Nowack B.; Ranville, J. F.; Diamond, S.; Gallego-Urrea, J. A.; Metcalfe, C.; Rose, J.; Horne, N.; Koelmans, A. A.; Klaine S. J. Potential scenarios for nanomaterial release and subsequent alteration in the environment. *Environmental Toxicology and Chemistry*. Vol. 31 (1) pp: 50-59. 2012
- Paper IV. Hammes, J.; Gallego-Urrea, J. A.; Hassellöv, M. Geographically distributed classification of surface water chemical parameters influencing fate and behavior of nanoparticles and colloid facilitated contaminant transport. *Water Research*. Vol. 47 (14) pp. 5350–5361. 2013
- Paper V. Gallego-Urrea J. A.; Hammes J., Cornelis G.; Hassellöv, M. Multimethod 3D characterisation of natural plate-like nanoparticles: shape effects on equivalent size measurements. Manuscript
- Paper VI. Gallego-Urrea J. A.; Hammes J., Cornelis G.; Hassellöv, M. Assessment of heteroagglomeration and sedimentation of gold nanoparticles in a set of characteristic European river water classes & seawater. Manuscript to be submitted to *Environmental Science and Technology*.
- Paper VII. Gallego-Urrea J. A.; Perez-Holmberg, J.; Hassellöv, M. Influence of different types of natural organic matter on titania nanoparticles stability: effects of counter ion concentration and pH. Manuscript to be submitted to *Environmental Science: Nano*.

## **Contributions to the papers**

Paper I. Major contributions to the writing process. Participated in the planning, sampling and measurements.

Paper II. Major contribution in the writing process.

Paper III. Participation in the workshop and writing of the environmental transformations section and bibliographic search.

Paper IV. Planning of the paper and contributions during the writing process.

Paper V. Planning of the experiments, performed some measurements, writing the paper.

Paper VI. Planning of the experiments, participated in some measurements, writing the paper.

Paper VII. Planning of the experiments, participated in some measurements, writing the paper.

## **Papers not included in the thesis**

Farkas, J.; Christian, P.; Gallego-Urrea, J. A.; Roos, N.; Hassellöv, M.; Tollefsen, K. E.; Thomas, K. V. Effects of silver and gold nanoparticles on rainbow trout (*Oncorhynchus mykiss*) hepatocytes. *Aquatic Toxicology* Vol. 96 (1) pp. 44-52. 2010

Farkas, J.; Christian, P.; Gallego-Urrea, J. A.; Roos, N.; Hassellöv, M.; Tollefsen, K. E.; Thomas, K. V. Uptake and effects of manufactured silver nanoparticles in rainbow trout (*Oncorhynchus mykiss*) gill cells. *Aquatic Toxicology* Vol. 101 (1) pp. 117-125. 2011

Farkas, J.; Peter, H.; Christian, P.; Gallego-Urrea, J. A.; Hassellöv, M.; Tuoriniemi, J.; Gustafsson, S.; Olsson E.; Hylland, K.; Thomas, K. V. Characterization of the effluent from a nanosilver producing washing machine. *Environment International* Vol. 37 (6) pp. 1057-1062. 2011

Ribeiro, F.; Gallego-Urrea, J. A.; Jurkschat, K.; Crossley, A.; Hassellöv, M.; Taylor, C.; Soares, M.V.M. A.; Loureiro, S. Silver nanoparticles and

silver nitrate induce high toxicity to *Pseudokirchneriella subcapitata*, *Daphnia magna* and *Danio rerio*. *Science of The Total Environment* Vol. 466–467 (1) pp. 232-241. 2014

## List of abbreviations

ALG	Sodium alginate
ASW	Artificial Seawater
CCC	Critical Coagulation Concentration
c-F <sup>3</sup>	Centrifugal-Field Flow Fractionation
DCS	Differential Centrifugal Sedimentation
DL	Diffusion Limited colloid aggregation
DLP	Dzyaloshinskii, Lifshitz, and Pitaevskii
DLS	Dynamic Light Scattering
DLVO	Derjaguin-Landau-Verwey-Overbeek
DOC	Dissolved Organic Carbon
EC	Electrical Conductivity
EDL	Electrical Double Layer
ENP	Engineered Nanoparticle
ESD	Equivalent Sphere Diameter
FA	Fulvic Acid
HA	Humic Acid
ICP-MS	Inductively-Coupled Plasma - Mass Spectrometry
IEP	Iso-Electric Point
IS	Ionic Strength
ISO	International Organization for Standardization
MNW	Model Natural Water
NM	Nanomaterial
NNP	Natural Nanoparticle
NOM	Natural Organic Matter
NP	Nanoparticle
NTA	Nanoparticle Tracking Analysis
OECD	Organization for the Economic Co-operation and Development
PB-E	Poisson-Boltzmann Equation
PCA	Principal Component Analysis
PEC	Predicted Environmental Concentration
pH <sub>PZC</sub>	Point of Zero Charge
PNEC	Predicted No Effect Concentration
PSD	Particle Size Distribution

RL	Reaction Limited colloid aggregation
SRFA	Suwannee River Fulvic Acid
SRHA	Suwannee River Humic Acid
TR-DLS	Time-Resolved Dynamic Light Scattering
vdW-Ld	van der Waals - London dispersion
WWTP	Wastewater treatment plant





# **1. Introduction and background**

## **1.1. Nanotechnology and the environment**

Nanotechnology, or the manipulation of objects in the scale of 1-100 nm, has attained great attention owing to the possibilities offered to solve many technological problems of today's society. Given the special characteristics at the nanoscale range, a number of promising applications of new materials is starting to become materialized in many scientific and industrial fields including environmental remediation, energy storage, solar energy collection, catalysis, improvement of electronic devices, medicine and development of more sophisticated analytical chemical instrumentation.<sup>1,2</sup>

The increase in manufacturing of consumer goods based on nanoparticles (NP) and nanomaterials (NM) has raised concerns about the possibility that these enter into the aquatic environment.<sup>3</sup> In the environmental risk of chemicals, predicted no effect concentrations (PNEC) are used as a rough estimate of the exposure level at which ecosystems will suffer no harm and predicted environmental concentrations (PEC), obtained from measurements or models, are estimates of the exposure levels. If the ratio PEC/PNEC is less than unity, then there will be a certain degree of confidence of a low environmental risk associated to the use of the chemical. This confidence level depends on the number of species tested, the timeframe of the predictions and the relevance of the species tested for the ecosystem.<sup>4</sup> Suitable platforms to evaluate the risks associated with the entrance of engineered NP (ENP) or NP released from products containing NM are lacking. One of the identified needs is establishing experimental and theoretical platforms that support the modelling of the environmental concentrations and exposure associated with NP in natural waters.<sup>5</sup>

## **1.2. What are nanomaterials and nanoparticles?**

Many of the novel properties of nanosized materials are dependent on, but not restricted to, their size and large specific surface area.<sup>6, 7</sup> Nanoparticles, from the environmental perspective, are a subset of the colloidal domain (1-1000 nm) and have been routinely defined as objects that have 3 dimensions in the range of 1-100 nm<sup>8</sup>. Nanoobjects, on the other hand, have 1 or more dimensions in this range. The definition in the ambit or risk assessment has been the focus of controversy in the US and Europe,<sup>9, 10</sup> a discussion that led to positions advocating to create a definition based on emerging special properties which ultimately would lead to more adaptive regulations.<sup>6, 11</sup> To facilitate their regulation, the European Commission adopted the recommendation on the definition of a nanomaterial<sup>12</sup> stating that a nanomaterial should contain 50% or more particles in the particle size distribution, PSD (including agglomerates), with one or more external dimension in the range 1 to 100 nm. This implies the necessity for measurement of particle number concentrations, ideally both from primary NP to their large aggregates (weakly bound assemblage of NP) and agglomerates (strongly bound assemblage of NP) that are generated through the various environmental fate processes.

Other categorizations of NP and NM have been suggested. Foss Hansen et al.<sup>13</sup> suggested to use categories based on the physical structure: (1) bulk NM, (2) surfaces of NM and (3) NP. NP are further divided in the sub-categories airborne, surface-bound, suspended in a liquid and embedded in a solid. Another suggestion to catalogue NM is based on the chemical composition:<sup>14</sup> (1) carbon-based NP such as fullerenes and carbon nanotubes, (2) metal oxide NP, such as titanium dioxide, (3) metallic NP, such as gold, (4) others, such as nanopolymers.

Some of these definitions are included as a starting point to outline the possible pathways of ENP and their transformation products in aquatic environments presented in Figure 1.

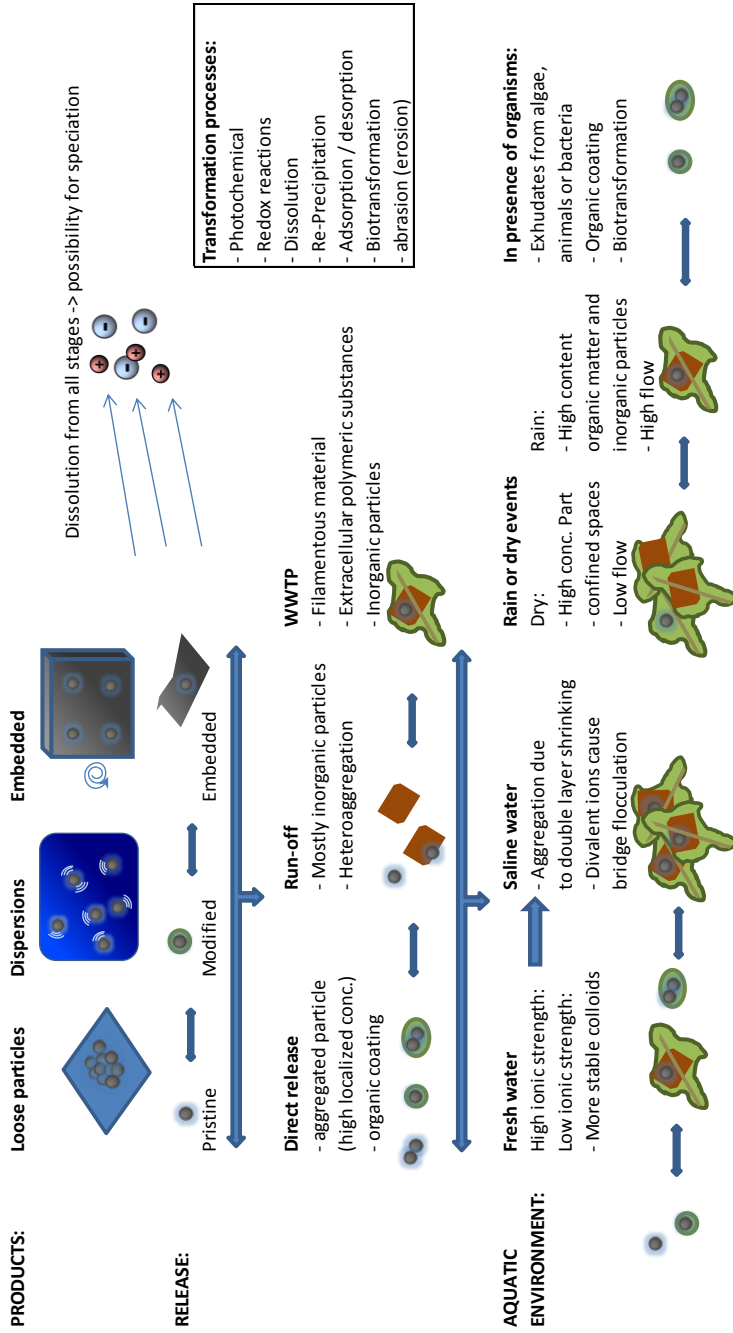


Figure 1. Schematic representation of the possible pathways for ENP release, transport and transformation in aquatic environments.

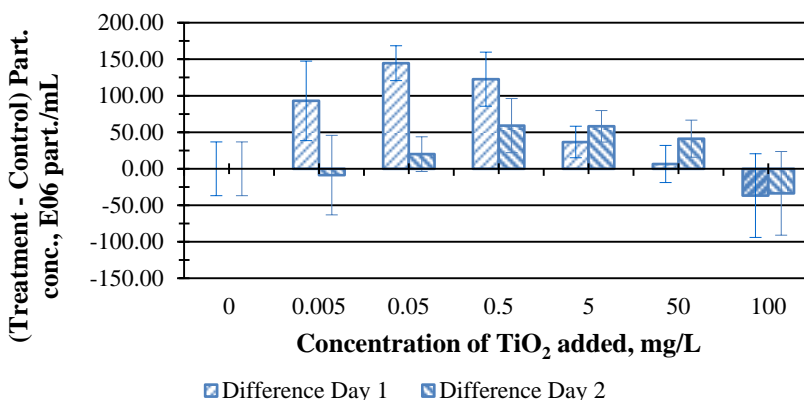
### 1.3. Environmental Nanosafety research

As the number of products containing nanomaterials (nanocomposites) and ENP increases, the possibility that particulate transformation residues<sup>15-17</sup> detached from NM or the ENP themselves<sup>18</sup> enter the aquatic environment grows with the consequent raise of possible new environmental hazards.<sup>19, 20</sup> Among the possible nano-specific hazards are included the possibility to cross membranes or other biological barriers<sup>21</sup>, deposition near biological entities leading localized high concentrations of hazardous materials and the transport of other contaminants attached to NP.<sup>22-25</sup>

The environmental risk assessment of these new materials involves the identification of associated hazards as well as the routes leading to exposure.<sup>4</sup> The analysis of the effects related to ENP exposure has proven to be a tough challenge.<sup>26-28</sup> This is in part due to the dynamic character of NP in aqueous environments where they are subject to external forces dependent on the water chemistry (pH, composition, dissolved gases and redox conditions), other physical factors (temperature, light exposure, shear gradients) and, often overlooked, NP number concentration and particles size distribution. Therefore, the exposure of organisms to NP is a dynamic variable that has to be carefully investigated in order to achieve a more thorough understanding of the environmental risk associated to these novel materials.<sup>28-31</sup> An example of the dynamic nature of ENP in ecotoxicity tests is presented in Figure 2 showing the variation in number concentration of particles found with nanoparticle tracking analysis, NTA, during a test for toxicity of TiO<sub>2</sub> NP towards fresh water algae.

The exposure assessment of any chemical, including ENP, can be separated into emission (the transfer between technosphere and environment) and fate or transport characterization. Emissions of ENP can occur in punctual or dispersed form with the consequent high or low concentration which in turn will influence the fate processes of the ENP. Emissions can be typified according to the temporal frame that the discharge occurs (periodical or continuous) or according to the path of the ENP to the aquatic environment (direct or indirect, e.g. via fumigation or wastewater treatment plant, WWTP, respectively).<sup>4, 32-35</sup> The extent to which these possible routes are likely points of entry for nanomaterials into the aquatic environment has been analyzed in great

detail for situations with full sanitation coverage and controlled waste disposal.<sup>36</sup> In Paper III some of these release scenarios are explored for a set of common NM.<sup>15</sup>



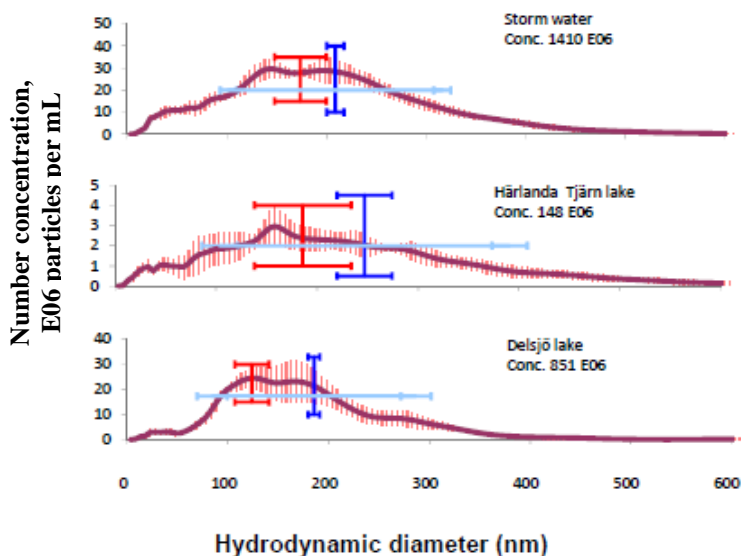
**Figure 2. Difference between the concentration of particles in the control and the concentration in each treatment for toxicity of TiO<sub>2</sub> NP towards fresh water algae (OECD 201 growth media; 72 hours exposure) followed with NTA. Concentrations measured correspond mostly to aggregates. Adapted from Paper II Gallego-Urrea, et al.<sup>37</sup>, with permission from Elsevier copyrights 2011.**

Fate processes refers to the transport, transformation and accumulation of a particular contaminant. In the case of ENP the transformations processes are more complex compared to regular chemical contaminants because the time-frame for achieving thermodynamic equilibrium, an underlying assumption for regular chemicals, is much larger than for ENP. The processes that can be relevant for ENP can include dissolution, aggregation, sedimentation, sorption, among others.<sup>15, 16</sup> These processes are highly related to the ENP characteristics, water chemistry (IS, NOM quantity and quality), hydrodynamic conditions (shear stress) and the presence of other interfaces (e.g. suspended solids, rocks, biofilms, and gas-water). The transport and accumulation of ENP comprises the mobility of the original or transformed ENP and this transport occurs simultaneously with the transformations processes. Traditional transport models rely on partition coefficients and these are established on the concept of achieved thermodynamic equilibrium.

Therefore, it has been argued that dynamic-transport models are more appropriate for describing the transport of ENP.<sup>29, 38, 39</sup> Two classical models, available from the literature on colloidal chemistry, are the

Derjaguin-Landau-Verwey-Overbeek (DLVO) theory<sup>40</sup> for evaluating the interaction potential between surfaces and Smoluchowski's<sup>41</sup> theories for diffusion and collisions. These models are capable of evaluating in a particle-particle base the interaction forces that lead to aggregation, agglomeration, break-up and sedimentation in a particle-particle base. Electrostatic repulsion and Van der Waals attractions are the main forces considered in these approaches but, in principle, they can be extended by empirical approximations to account for other forces (e.g. steric hindrance, depletion forces) and media interactions (e.g. shear forces, attachment efficiencies).<sup>29</sup>

Suspended solids are ubiquitous material in rivers and other water bodies<sup>42</sup> and can interact with released ENP.<sup>43-46</sup> These can be categorized based on their size in sand, silt, clay and colloids;<sup>42</sup> a portion of the clay fraction (<3  $\mu\text{m}$ ) and the colloidal fraction (typically <1  $\mu\text{m}$ ) comprise the natural NP (NNP).<sup>47-49</sup> This small natural particulate matter is heterogeneous spanning from inorganic clays<sup>50</sup> to organic macromolecules (natural organic matter, NOM).<sup>51</sup> It has been claimed that the overwhelming presence of suspended and colloidal matter compared to the predicted smaller number concentrations of ENP in the environment will play a major role in the final fate of ENP via heteroaggregation, a process that could lead to the formation of larger aggregates.<sup>43-46</sup> Other types of NP that can be found in the aquatic environment are unintentionally produced NP coming from the weathering of man-made products (i.e. not nanocomposites).<sup>52</sup> In Paper I the amount and PSD of NNP in several natural waters around Gothenburg, Sweden were analyzed using Nanoparticle Tracking Analysis (NTA). Figure 3 presents an example of PSD for storm water and two small lakes.



**Figure 3. PSD and number concentrations (particles per mL) of NNP in three sampling locations in Gothenburg, Sweden, measured with NTA. Adapted from Paper I with permission. Gallego-Urrea et al<sup>47</sup>, copyrights CSIRO publishing 2010.**

Some knowledge gaps in the environmental risk assessment of ENP have been identified<sup>3, 5, 53, 54</sup> including the development of analytical methods to track ENP in complex matrices, the development of structure-activity relations to predict the toxicity and fate of NP, the development of models for release and exposure scenarios and, more recently, the adaptation of transport and fate models to account for the generation of NP from dissolved metals, the release of NP from larger solids, and to gain knowledge about the role of ENP in chemical equilibrium modelling.<sup>5</sup> Some of the knowledge on these issues has advanced significantly as the field has evolved, e.g. identification of NP in complex matrices<sup>37, 55, 56</sup> and the factors contributing to hazard of ENP. However, despite the advances done in hazard assessment the relation to aquatic exposure is still highly uncertain since the fate of ENP in ecotoxicological studies is dependent on the initial conditions used (e.g. particle PSD, number concentration, mixing and media composition). Consequently, the NP fate in real situations and the resulting environmental concentrations and PSD can differ from the conditions tested in ecotoxicological studies.

The uncertainty associated with measuring composition and number of NNP and colloids in natural waters is of high importance because interactions between these and released ENP are critical for the final fate of ENP. Further, exposure assessment tools that can be used to predict environmental concentrations are lacking.<sup>35, 36</sup> Processes occurring in the environment are not very well parameterized and require platforms that help to integrate measurements chemical equilibrium models.<sup>5</sup>

## **1.4. Aim and approach**

The overall aim of this thesis is the development of tools that can be used to determine or predict the aquatic environmental concentrations of ENP and, consequently, the exposure of these to organisms. Fate processes can be investigated in different ways ranging from mechanistic studies performed in pure water with only one or two chemical components such as single electrolytes or NOM to sampling studies with complex media such as natural water samples. Mechanistic studies aim to identify factors that control processes and gain quantitative data while sampling studies aim to be highly relevant for the behavior of particles under real natural conditions.

Studies performed under simplified conditions are reproducible and valuable to identify the relevance of single processes, but are only valid for the limited set of hydro-chemical conditions and lack the ability to predict complex interactions between the whole water body components and NP. In contrast, experiments with natural waters approach real conditions but they are prone to be affected by seasonal and local variations increasing the complexity and the amount of unknown parameters which precludes the judicious interpretation of the underlying environmental processes.

For emerging contaminants, such as ENP, the situation is more complex owing to the non-stationary behavior, the intrinsic heterogeneity of physicochemical parameters and the likelihood of being transformed in the environment.

Given these appreciations, the approach in the development of this work was to build up from mechanistic studies moving onto more complex standardized test systems that resemble relevant environmental aspects to a higher extent.



To accomplish this aim the following results were achieved following the approach methodology described above:

- Development of nanoparticle tracking analysis, NTA, applications for evaluating PSD and number concentrations evolution in aqueous suspensions for Au NP (Paper I and Paper VI), TiO<sub>2</sub> NP (Paper II), and NNP in contrasting natural samples (Paper I) and anisometric clay illite particles (Paper V).
- Characterization of a suspension of anisometric clay illite particles to be used as a model colloid in fate studies (Paper V).
- Parameterization of fate processes, specifically aggregation behavior and stability ratios of TiO<sub>2</sub> NP (Paper VII) under different ranges of pH, electrolytes concentration and valence and presence of contrasting sources of NOM.
- Compilation of theoretical frameworks for the aquatic fate of ENP in the aquatic environment for potential transformation of ENM (Paper III), for stability parameters due to electrolyte concentration (Paper IV) and for theoretical approaches in exposure assessment of aquatic ENP (this work).
- Development of test platforms for the evaluation of fate processes of ENP in river waters by generating a set of European model natural waters, MNW (Paper IV), and evaluating the heteroaggregation and sedimentation of Au NP and illite in these MNW (Paper VI).
- Critical analysis of time-resolved dynamic light scattering, TR-DLS, for the evaluation of aggregation rates for Au NP (Paper VI) and for TiO<sub>2</sub> NP (Paper VII).



## 2. Nanoparticle characteristics

NP can be classified according to certain key parameters that will define the fate processes in aquatic environments. Some key properties are material, size, shape, surface coating or functionalization and surface charge.<sup>57</sup> These characteristics will define to which extent the fate processes will affect the environmental concentrations of ENP.

### 2.1. Nanoparticle size and equivalent diameter

Particle size is one of the most important parameters in ENP exposure assessment because many key particle properties, fate processes and biological uptake vary with size. It is customary to express the diameter as an equivalent spherical diameter (ESD). Some of the most common ESD and their definitions are listed in Table 1. Many of these definitions are used throughout the thesis and in the papers.

Other equivalent particle diameters can be specified depending on the context or type of measurement or specific aim. Some notorious examples are **radius of gyration** and **equivalent rotational diameter**. Other ESD could be defined for certain purposes if required, e.g. **equivalent light scattering diameter**.

### 2.2. Nanoparticle shape

Particle shape is a very important factor that can influence the uptake and effects of NP,<sup>58</sup> their physical properties<sup>59</sup> and also their fate.<sup>60</sup> In terms of shape, particles can be described as anisometric particles (solid with different geometrical lengths in any direction, i.e. high aspect ratio),<sup>8</sup> as irregular isometric (similar to spheres), as branched, spiky or dendritic particles, or as hollow or porous structures.<sup>61</sup>

Anisometric particles can often be described with an equivalent geometrical shape that can be more easily mathematically described. For instance, nanotubes can be modelled as cylinders or prolate spheroids for determining their hydrodynamic diameter<sup>62</sup> or light scattering

properties.<sup>63</sup> Similarly, nanoplates can be described as disks (short cylinders) or oblate spheroids (See Paper V).

**Table 1. List of common equivalent spherical diameters**

Description	Formula	Eq.
Volume-equivalent diameter or the diameter of a sphere with the same volume or mass.	$d_v = \sqrt[3]{\frac{6 \cdot V_p}{\pi}}$	1
Hydrodynamic equivalent diameter or the diameter of a sphere with the same friction coefficient, as defined by the Stokes-Einstein equation.	$d_H = \frac{k_B \cdot T}{f} = \frac{k_B \cdot T}{3 \cdot \pi \cdot \mu \cdot D_T}$	2
Stokes or settling equivalent diameter or the diameter of a sphere with the same settling velocity.	$d_s = \sqrt[2]{\frac{d_v^3}{d_H}} = \sqrt[2]{\frac{18 \cdot \mu \cdot v_s}{(\rho_p - \rho_f) \cdot g}}$	3
Surface-area-equivalent diameter or the diameter of a sphere with the same surface area:	$d_A = \sqrt[2]{\frac{6 \cdot A_p}{\pi}}$	4

Notes:

In equation 1  $V_p$  is the volume of the particle.

In equation 2  $k_B$  is the Boltzmann constant ( $1.38 \times 10^{-23} \text{ m}^2 \cdot \text{kg} \cdot \text{s}^{-2} \cdot \text{K}^{-1}$ ),  $T$  is the absolute temperature,  $f$  is the friction coefficient which has been replaced in the last term for the Stokes drag's friction factor ( $f=3 \cdot \pi \cdot \mu \cdot D_T$ ),  $\mu$  is the dynamic viscosity of the medium and  $D_T$  the translational diffusion coefficient averaged for all orientations.

In equation 3  $v_s$  is the steady-state settling velocity,  $\rho_p$  and  $\rho_f$  are the particle and fluid densities, respectively, and  $g$  is the standard acceleration of gravity ( $9.81 \text{ m/s}^2$ ).

In equation 4  $A_p$  is the surface area of the particle.

The decrease in hydrodynamic diameter and solvation for a particle that differs from a sphere with the same  $d_v$  can be expressed in function of the corresponding friction factor:<sup>64</sup>

$$\frac{f}{f_0} = \frac{f}{f^*} \frac{f^*}{f_0} \quad 5$$

Where  $f_0$  is the friction factor of the unsolvated sphere,  $f^*$  is the friction factor of a spherical particle with the same volume as the solvated particle and  $f$  is the friction factor of the actual particle.

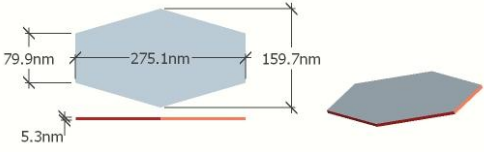
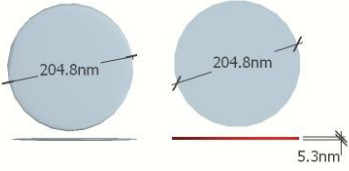

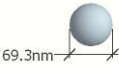
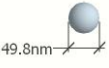
Solvation can also be very important in the determination of the settling velocities of small and dense particles, since the effective density of the solvated particle will be reduced due to the water in the hydration layer. This effect has been reported for citrate-coated AuNP of 30 nm in diameter with an apparent density of approximately 76% of the bulk density of gold<sup>65</sup> which, if related to hydration only, corresponds roughly to a solvated water layer of 1.5 nm.

To illustrate the effect of particle shape on the equivalent diameters it is possible to use the illite clay particle from Paper V. A formula for calculating the hydrodynamic diameter of oblate spheroids was derived finding the friction coefficient using creeping motion equations valid for very low Reynolds numbers and assuming random orientation of the particles (i.e. coincident center of mass, buoyancy and hydrodynamic effect so that no specific movement direction is favored)<sup>66</sup> and replacing in equation 2.

$$d_H = \frac{8 \cdot d_p \cdot (1 - \phi^2)^{3/2}}{-(2 \cdot \phi^2 - 3) \cdot \arcsin(\sqrt{1 - \phi^2}) + (1 - 2 \cdot \phi^2) \cdot \arctan(\sqrt{1 - \phi^2} / \phi)} \quad 6$$

where  $d_p$  is the major diameter and  $\Phi$  is the ratio between the minor and major diameter of an oblate spheroid approximating the plate-like illite particles. This result is exactly equivalent to those found by Jennings and Parslow<sup>62</sup> The results illustrating the differences between the different equivalent diameters are presented in Table 2.

**Table 2. Scaled drawing of a typical illite particle and approach used to obtain corresponding equivalent sphere diameter. Adapted from Paper V.**

Schema	Description
	<p>Example of original particle with irregular shape showing the major dimensions. Thickness, <math>H_p</math>, 5.3 nm.</p>
	<p>Upper and lateral views of the equivalent spheroid (left) and cylinder (right) with same projected area as the original particle and the corresponding plate diameter (<math>d_p = 204.8</math> nm) and <math>H_p</math>.</p>
	<p>Sphere with the same friction coefficient as the original particle. Hydrodynamic diameter, <math>d_h</math>. Eq 4.</p>
	<p>Sphere with the same volume as the original particle. Volume equivalent diameter, <math>d_v</math>. Eq. 1</p>
	<p>Sphere with the same settling terminal velocity as the original particle. Settling (Stokes) equivalent diameter, <math>d_s</math>. Eq 3.</p>

In Paper V the characterization of the illite particles confirmed the values found for the hydrodynamic diameter. The centrifugal techniques (centrifugal-Field Flow Fractionation, c-F<sup>3</sup> and differential centrifugal sedimentation, DCS) were, however, performing under the limit of detection in terms of separation capacity, probably due to the low equivalent Stokes diameter.

The surface roughness, porosity and branching of the particles is also important in terms of forces acting on the particle, the equivalent  $d_H$ , the reactive surface area and available reactive sites (patches or exposed crystal facets).

So far, the relation between different size measurements has only been discussed for hard nanoparticles, i.e. particles that are not flexible. The flexibility of a particle can give rise to extra forces that are more difficult to describe in simple mathematical terms. For some of these flexible materials, it is customary to use the term soft nanoparticle for organic particles or biological structures which bare a charge, e.g. humic acids and polysaccharides.<sup>67</sup>

Aggregates of colloidal particles usually have a fractal porous and/or branched structure that can be defined as:<sup>68</sup>

$$i = k_f \cdot \left(\frac{d}{d_0}\right)^{D_f} \quad 7$$

Where  $i$  is the number of particles in the cluster,  $k_f$  is a factor that depends on the type of diameter being calculated,  $D_f$  is the fractal dimension and  $d$  and  $d_0$  are the diameters of the cluster and the original particle, respectively.

### 2.3. Number concentrations and particle size distribution

NP in dilute suspensions can be characterized by its PSD as histograms of the frequency or number of particles within a given diameter range. The frequency can be more precisely called a probability distribution function (PDF),  $q_i$ , and the PSD will be formed by the pair  $(d_i, q_i)$  with  $d_i$  the equivalent diameter for each  $i$ -th size class.<sup>69</sup>

$$q_i(d_i) = \frac{n_i \cdot d_i^r}{\sum_i n_i \cdot d_i^r} \quad 8$$

Where  $r$  indicates the type of distribution.  $r$  can take values of 0 for number-weighted distributions (e.g. from counting methods), 1, 2 and 3 for length-, surface- and volume-weighted distributions, respectively.

Statistical mean values can be calculated accordingly:<sup>69</sup>

$$\overline{d}_k = \left( \frac{\sum_i d_i^k \cdot d_i^r \cdot n_i}{\sum_i d_i^r \cdot n_i} \right)^{1/k} \quad 9$$

With  $k$  denoting the type of average (-1 for harmonic mean, 0 for geometric mean, 1 for arithmetic mean, 2 for quadratic mean, etc.). Moment and moment-ratio notation can be used to generate mean values and variances as well with the advantage that results obtained from different techniques can be combined to obtain more simple mean statistics.<sup>69</sup>

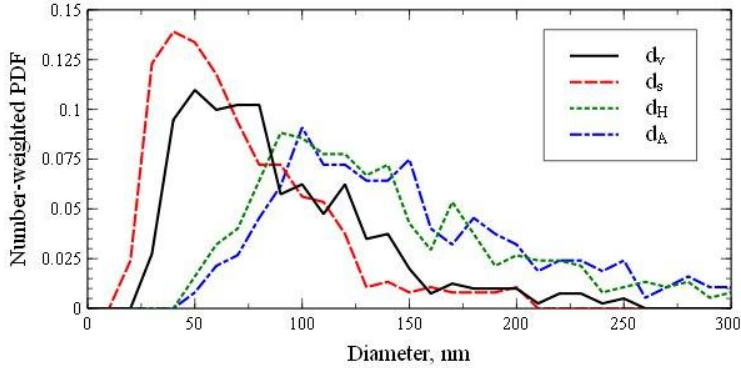
Other basic statistic parameters that can be used to characterize the PSD are: quantiles, median, mode, variance, skewness and kurtosis. In Paper I and Paper II the PSD has been characterized using an arithmetic average of the number concentrations resulted from NTA measurements and averaged between measurements (Figure 3).

### ***Shape effects on equivalent PSD and average size of illite***

To illustrate the effect of shape on the different average values, the data from Paper V can be used. In this case the heights and characteristic length of clay particles were measured with atomic force microscopy (AFM). 374 particles were measured and the corresponding  $d_s$ ,  $d_v$ ,  $d_H$  and  $d_A$  were calculated with the equations 3, 1, 2 and 4, respectively. The corresponding number-weighted arithmetic averages were 66, 84, 139 and 153 nm. The corresponding PSD are presented in Figure 4.

The PSD of illite particles in Figure 4 indicates that  $d_H$  and  $d_A$  follow a similar trend and the same is valid for  $d_s$  and  $d_v$ . However, for these high-aspect particles the differences between  $d_H$  and  $d_A$  compared to  $d_s$  and  $d_v$  are considerable large (almost 2 times). This is a particularly important feature for characterizing NP and understanding the significance of the different physical parameters obtained with different analytical techniques.





**Figure 4. PSD of 374 illite particles measured with AFM and converted to the equivalent spheres diameters.**

The number concentration of a suspension can be calculated as:

$$N = \frac{\sum_i n_i}{V_T} \quad 10$$

where  $V_T$  is the total volume of the liquid containing the particles. The volume fraction,  $\varphi$ , is often used to characterize colloidal suspensions:

$$\varphi = \frac{\sum_i n_i \cdot V_i}{V_T} = \frac{\pi/6 \sum_i n_i \cdot d_{v,i}^3}{V_T} \quad 11$$

where  $V_i$  is the volume of the  $i$ -th particle. If the mass composition of all particles is the same, the mass concentration would be  $C = \rho \cdot \varphi$  with  $\rho$  the density of the material.

Number concentrations are very important in determining many of the fate processes acting on the ENP, particularly the processes of aggregation and agglomeration.<sup>29</sup>

## 2.4. Surface charge

Environmental fate of ENP will be highly influenced by the surface charge that they acquire in the water compartment. Surface charges can originate from hydroxylation of oxide surface groups (dependent on pH),

preferential adsorption of ions (e.g.  $I^-$  on AgI sols), dissociation of surface groups (like in NOM), isomorphic substitution (leading to permanent charges as in clays), adsorption of polyelectrolytes or accumulation of electrons (as in metallic particles).<sup>64</sup>

The surface charge of a NP will determine the extent of the repulsive electrostatic force between particles which is one of the main forces stabilizing NP in suspension.<sup>70</sup> If the surface charge is strongly dependent on pH (which is the case for metal oxides) then the pH of the receiving water body is critical for the final fate of ENP. The isoelectric point (IEP) of a metal oxide particle is usually expressed as the pH value where there is no net electrophoretic mobility (point of zero charge,  $pH_{PZC}$ , contrastingly, is the pH value where the net charge of the surface is 0). If the pH of a suspension is close to the IEP there electrostatic stabilization will be negligible, as it will be seen ahead.

If the surface potential is determined by any other mechanism, then the nature of the ionic composition needs to be carefully looked upon in order to be aware of the presence of potential determining ions or possible ion-ion correlations.<sup>71, 72</sup>

Surface charge is usually expressed in terms of the  $\zeta$ -potential,  $\zeta$ , or the potential located near the shear layer a few ångströms (Å) away from the particle surface. It is usually determined by measurements of the electrophoretic mobility,  $u$ . Henry's equation can be used to convert electrophoretic mobility to zeta potential.

$$u = \frac{2 \cdot \epsilon \cdot \epsilon_0 \cdot \zeta \cdot F(\kappa \cdot a)}{3 \cdot \mu} \quad 12$$

where  $\epsilon$  is the relative permittivity for the medium (80.1 at 293K),  $\epsilon_0$  is the permittivity for vacuum ( $8.85 \times 10^{-12} \text{ C}^2/\text{J.m}$ ),  $\mu$  is the dynamic viscosity of the medium and  $F(\kappa a)$  is a function that varies between 1 and 1.5 in order to account for the assumptions of Henry or Schmolokowski electrophoretic equation<sup>64</sup>.  $F(\kappa a)$  can be found by Ohshima's approximation<sup>73, 74</sup> with  $\kappa$  the Debye-Hückel parameter defined as:

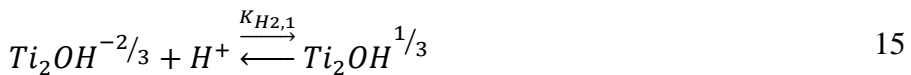
$$\kappa = \sqrt{\frac{\sum_i ((n_i)_0 \cdot z_i^2) \cdot e_0^2}{\varepsilon \cdot \varepsilon_0 \cdot k_B \cdot T}} \quad 13$$

where  $(n_i)_0$  is the concentration of the  $i^{th}$  ion in the bulk phase,  $z_i$  is its valence and  $e_0$  is the elementary charge ( $1.602 \times 10^{-19}$  C).

The Debye-Hückel parameter, also called the inverse Debye length, is a recurrent variable in the derivations of interaction potentials between charged surfaces. Because of the dependency of the electrostatic interactions on the Debye length, this is sometimes referred as the extension of the electrical double layer, EDL.<sup>40</sup>

### *Surface complexation of titania (TiO<sub>2</sub>)*

In Paper VII the interactions of anatase TiO<sub>2</sub> NP with pH, different electrolytes and different types of organic macromolecules was evaluated. Both anatase and rutile have amphoteric surfaces that follow the Pauling concept.<sup>75</sup> The titania structure is a Ti<sup>4+</sup>-filled oxygen octahedra. The oxygens in the bulk of the solid are triply coordinated (Ti<sub>3</sub>O<sup>0</sup>) while the surface oxygens can be singly (TiO<sup>-4/3</sup>), doubly (Ti<sub>2</sub>O<sup>-2/3</sup>), and triply coordinated (Ti<sub>3</sub>O<sup>0</sup>). The proton affinity of the TiO<sup>-4/3</sup> group is high and once in water it immediately changes into TiOH<sup>-1/3</sup>, which may adsorb a second proton depending on the pH of the solution. The protonation reactions for singly and doubly coordinated surface groups can be given as:<sup>75</sup>



Assuming equal values for the constants of protonation of the titanium oxide surface,  $K_{H1,2}$  and  $K_{H2,1}$ , it can be shown that  $\log K_H = pH_{PZC}$  in the case of symmetrical ion pair formation<sup>75</sup>. In the presence of electrolytes, the hydrated ions will form ion pairs with surface hydroxyls as outersphere complexes without forming strong chemical bonds with the surface groups. At any given pH, cations will react with the available negatively charged titania surface groups (TiOH<sup>-1/2</sup> and Ti<sub>2</sub>OH<sup>-2/3</sup>) and

anions with the positive surface groups ( $\text{TiOH}^{2/3}$  and  $\text{Ti}_2\text{OH}^{1/2}$ ). The lyotropic sequence (Hofmeister series) differs between monovalent and divalent ions. Binding increases with increasing ion size for earth alkali ions, whereas the differences in the affinity for the surface occur in the inverse direction for alkali ions. Therefore, not only the electrostatical forces are in place but monovalent and bivalent cations can adsorb by different mechanisms.<sup>76</sup>

## 2.5. Surface coating

ENP are often composed of different layers depending on the purpose or the origin of the NP. For ENP, internal inorganic layers can be present as an integral part of the nanocomposite. Some ENP are provided with organic coatings onto the surface from the manufacturing process to provide stability, facilitate particle dispersion in a matrix or provide a certain function. Stability of functionalized ENP can be due to steric repulsion but also some electrostatic interaction can play a role if the organic coating carries a charge<sup>77</sup> or the surface of the core particle still provides part of its charge for electrostatic repulsion.<sup>78</sup> ENP coated with polymers can also be prone to aggregation either by affinity of the polymer to another uncoated surface<sup>79</sup> or by bridging with certain types of NOM. The quality of the coating can also make a difference on the uptake and effects of ENP in organisms.<sup>80</sup> The degradation of the particle coating has also been shown to have effects on the final fate of ENP.<sup>81</sup>

### *Sorption of organic substances*

It has been observed that for polyelectrolyte adsorption on surfaces the low critical adsorption Gibbs energy,  $\Delta g_{\text{ads-crit}}$ , required to surpass to overcome the entropy loss upon attachment is about 0.2–0.4  $k_B \cdot T$  per segment. Those low Gibbs energies are easily obtained for organic matter. For instance, the Gibbs energy for the hydrophobic bonding of one  $\text{CH}_2$  segment to a hydrophobic patch on a surface is already about 1  $k_B \cdot T$ . For this reason polyelectrolytes tend to form several layers of adsorbed substance and overcharging can take place.<sup>76</sup> The sorption of NOM onto the surfaces of organic coatings, either during manufacturing or as a natural process, has been shown to be very important for providing steric or electrostatic stability to the particles or to destabilize them by a so-called bridging effect as will be shown below.

### 3. Theoretical framework for particle fate

#### 3.1. Brownian diffusion

##### *Thermodynamic description of diffusion:*

If external forces can be neglected, the composition of a single equilibrium phase will be macroscopically uniform throughout. This means constant concentration in the phase, macroscopically speaking.

Fundamentally, it is the second law of thermodynamics that is responsible for the uniform distribution of matter at equilibrium since entropy is maximum when the molecules are distributed randomly throughout the space available for them (2<sup>nd</sup> law: the entropy of an isolated system which is not in equilibrium will tend to increase over time, approaching a maximum value at equilibrium).

The resulting transport of matter from a populated place to an unpopulated place is called diffusion. Ficks's first law introduces the term for diffusion coefficient of the solute describing the flux of material,  $J$  in units of mass per area and time, as:

$$J(x, t) = -D \frac{\delta C(x, t)}{\delta x} \quad 16$$

where  $D$  is the diffusion coefficient of the solute, in units of square length per unit of time.  $C$  is concentration of the solute and  $x$  is the distance in the direction of the material flow.

##### *Diffusion coefficient and friction factor:*

A very general way to describe a force is to write it as the negative gradient of a potential. In the context of diffusion, the potential to be used is chemical potential  $\mu_i$ , the partial molal Gibbs free energy of the component of interest.<sup>64</sup> Thus, the magnitude of the driving force (per particle) diffusion may be written as

$$F_{diff} = -\frac{1}{N_A} \frac{\delta\mu_i}{\delta x} \quad 17$$

This is called the thermodynamic force for diffusion. It is necessary to divide by the Avogadro's number  $N_A$  since  $\mu_i$  is a molar quantity. Thermodynamics shows that the chemical potential is defined by:

$$\mu_i = \mu_i^0 + N_A \cdot k_B \cdot T \cdot \ln(a_i) = \mu_i^0 + N_A \cdot k_B \cdot T \cdot \ln(\gamma_i \cdot C_i) \quad 18$$

where  $a_i$ ,  $C_i$ , and  $\gamma_i$  are the activity, concentration and activity coefficient, respectively, of the  $i$ -th component. For infinite dilutions the activity coefficient may be assumed to be 1. Substituting equation 18 into equation 17 gives:

$$F_{diff} = k_B \cdot T \frac{\delta \ln(C_i)}{\delta x} = \frac{k_B \cdot T}{C} \frac{\delta C_i}{\delta x} \quad 19$$

This force will be equal to the force of viscous resistance under stationary state conditions, given by  $F_v = f \cdot v$  where  $f$  is the friction factor and  $v$  is the stationary state velocity in units of length per time. The magnitude of the velocity of diffusion equals:

$$v_{diff} = -\frac{k_B \cdot T}{f \cdot C} \frac{\delta C}{\delta x} \quad 20$$

Where the subscript is omitted from the concentration of the solute  $C$  because this is now the only quantity involved in the relationship. Finally, the flux of material by definition equals the product of its concentration and its diffusion velocity:

$$J = C \cdot v_{diff} \quad 21$$

Combining equations 20 and 21 and comparing with equation 16 leads to the Stokes-Einstein relation presented in equation 2.

***Brownian motion and diffusion:***

A liquid that is totally homogeneous on a macroscopic scale undergoes continuous fluctuations at the molecular level. As a result of these fluctuations, the density of molecules at any position in the liquid fluctuates with time and at any time fluctuates with location but the mean density of the sample has its bulk value. This will cause varying pressures on the surface of any particle submerged in the liquid and the particle will move due to the force variation on its surface. The pattern of displacement will be random and the bigger the particle, the smallest the effect of the small pressure variations.

This phenomenon was first studied microscopically with pollen seeds of approximately 800 nm and was described by the British biologist Robert Brown in 1866.<sup>82</sup> The relation connecting Brownian motion and the diffusion coefficient was derived by Einstein and Smoluchowski simultaneously. It is possible to use a comparison between the one-dimension random walk statistics and the movement of a particle. The walk statistics is used as a model to find where a particle is going to move in a one-dimension length during a certain amount of time by random motion. The final result is an expression relating the root mean square of the distance traveled by a particle to the diffusion coefficient:<sup>64</sup>

$$\overline{x^2} = 2 \cdot D \cdot t \quad 22$$

Or for three dimensional movement

$$\overline{x^2} + \overline{y^2} + \overline{z^2} = 6 \cdot D \cdot t \quad 23$$

This diffusion coefficient is related only to Brownian motion and it is not related to other interactions like particle-particle relations. Therefore, it's called self-diffusion coefficient that might differ from the actual bulk diffusion coefficient for concentrated systems.

Incidentally, the root mean square displacement, evaluated from a statistically meaningful number of observations, permits this translational  $D$  to be calculated and this principle is used by nanoparticle tracking analysis NTA and explained in Paper I and Paper II.

## 3.2. Colloidal stability

The van der Waals - London dispersion (vdW-Ld) interaction is the universal, long range, interaction that is ubiquitous to all materials and is originated from the resulting fluctuating electromagnetic field generated from the interaction of dipoles.<sup>83</sup> The forces that arise can be attractive or repulsive depending on the configuration of the surfaces system.

The vdW-Ld interactions usually generate attractive forces in aqueous suspensions which can be calculated using the Hamaker coefficients. A Hamaker coefficient is a property of the material that encompasses London dispersion forces, Debye forces and Keesom forces which are all originated by the polarizability of the constituent atoms of the system and the consequent fluctuations of the electromagnetic field between them. Non-retarded Hamaker constant is the value at short distances when the time required for the electromagnetic interaction between the two surfaces can be neglected. The full spectral Hamaker coefficient, coming from the continuum theoretical approach of Lifshitz (or DLP) theory,<sup>84, 85</sup> is a function of the separation distance from the surface where electromagnetic retardation takes place. The effect of ions in solution is also important because these screen the electromagnetic interaction due to charge-fluctuation<sup>85</sup>.

Electrostatic forces arise when the non-specific ions (i.e. ions that do not have specific affinity for the material surface) are “ordered” next to the surfaces due to the electrical potential forming a so-called electrical double layer (EDL). These arrangements of counter-ions and co-ions generate an osmotic deficit that results in a force that is directed in the opposite direction of both surfaces (repulsion). This repulsive force can be derived mathematically by a number of approximations that depends on the way to solve the Poisson-Boltzmann equation (P-BE). The linearized P-BE is the most used for deriving the solutions and this implies that the surface potentials are low (<25 mV) and that the internal electrical fields are neglected. Linear superposition approximation is a good approach for large separation distances.<sup>86</sup> Another approximation that can be applied is the Derjaguin approximation which gives good results for small separation distances. The assumption of constant surface charge or constant surface potential needs to be done when solving the electrical forces by using the Helmholtz free energy approach.<sup>87</sup> Since flocculation occurs at low distances, the Derjaguin



approximation is adequate for calculating theoretical stability ratios (or inverse aggregation efficiencies).

The sum of attractive and repulsive potentials as a function of distance between the surfaces of two particles will determine the tendency for aggregation and duplet formation:

$$V_T(\kappa \cdot H) = V_R(\kappa \cdot H) + V_A(\kappa \cdot H) \quad 24$$

Where  $V$  is the potential usually expressed dimensionless in scaled  $k_B T$  units and the subscripts  $T$ ,  $R$  and  $A$  stand for total, repulsive and attractive, respectively. The potentials are a function of the dimensionless distance  $\kappa \cdot H$  with  $\kappa$ , the inverse Debye length defined previously (equation 13), and  $H$  the interparticle distance.

If only electrostatic repulsive interactions and Van der Waals attractive forces are considered, the total interaction potential (known in this form as DLVO-potential) is thus a function of the Hamaker coefficient, the particles diameter, the surface potentials, temperature and the electrolyte valence and concentration. Because of the nature of these two forces the resulting potential can contain one or two maxima values, known as energy barriers, and one or two minima known as primary and secondary minimum. An example of the interaction potential for  $\text{TiO}_2$  spheres of 20 nm in diameter (like those used in Paper VII) is presented in Figure 5.

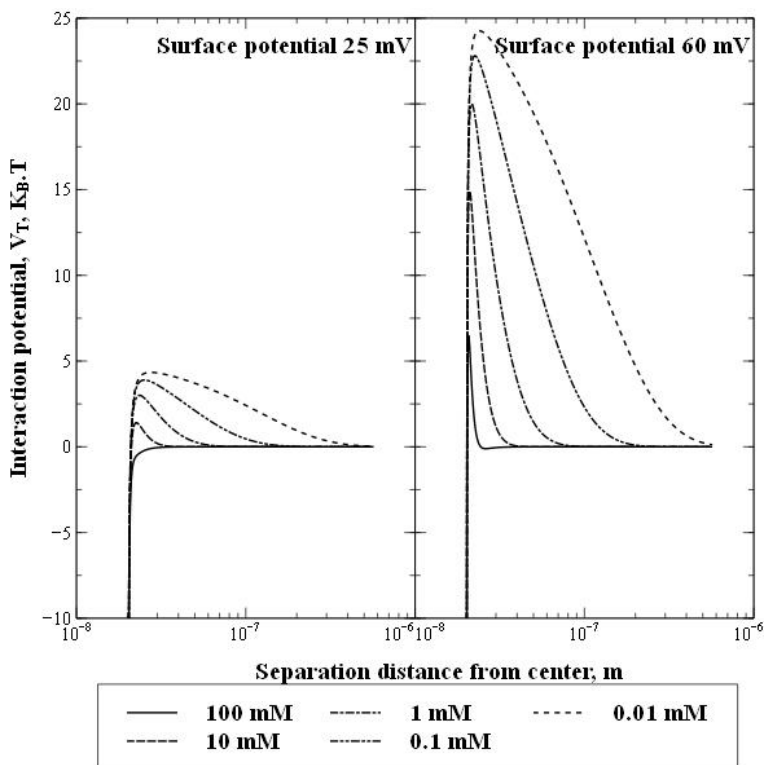
It is possible to observe that at 100 mM of monovalent electrolyte the particles with 25 mV surface potential are destabilized while the same type of particles with 60 mV surface potential still possess a significant interaction potential ( $> 5 K_B \cdot T$ ). This destabilization was also observed for bare  $\text{TiO}_2$  NP in Paper VII when the pH was closer to the IEP.

By finding the maximum value of the first energy barrier (closest to  $H=0$ ) it is possible to estimate the order of magnitude of the stability ratio,  $W$ , or inverse collision efficiency,  $\alpha$ , by using the approximation:<sup>40</sup>

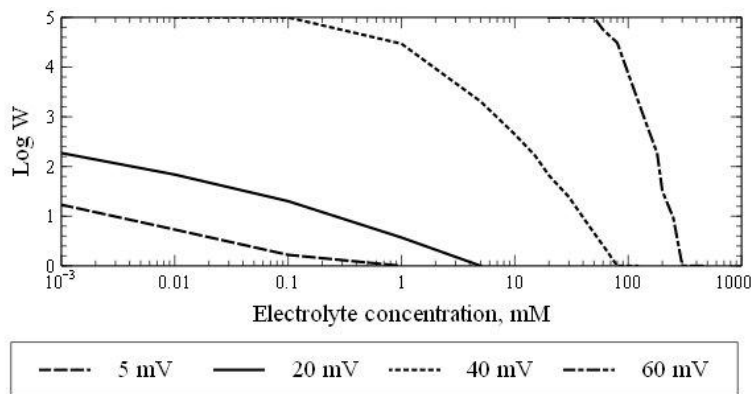
$$\frac{1}{\alpha} = W = \frac{1}{\kappa \cdot (a_i + a_j)} \cdot \exp\left(\frac{\phi_{max}}{k_B \cdot T}\right) \quad 25$$

Where  $a_i$  and  $a_j$  are the radii of the particle  $i$  and  $j$ , respectively and  $\Phi_{max}$  is the height of the energy barrier. For this equation it is assumed that the major contributions to the interaction potential come from the proximity of the maximum potential.

In Paper VII calculations were done using the Derjaguin approximation as a function of monovalent electrolyte concentration for equal-sized spherical  $\text{TiO}_2$  NP of 20 nm in diameter and varying surface potential (5, 20, 40, 60 mV). The results are presented in Figure 6.



**Figure 5. DLVO calculations for  $\text{TiO}_2$  using Derjaguin approximation. The different concentrations of monovalent electrolyte (symbols) and surface potentials (25 and 60 mV) are presented.**



**Figure 6. Theoretical stability ratios,  $W$ , as a function of electrolyte concentration, between two  $\text{TiO}_2$  spheres of 20 nm diameter found with equation 27 after determining the height of the energy barrier using Derjaguin approximation. The curves are truncated in  $\log(W)$  5 and 0 to allow better visualization.**

Hamaker constants can be evaluated more thoroughly for a complete quantitative treatment using continuum theory and it should be encouraged to evaluate as such for more complex nanoparticulate systems (e.g. complex shape or nanocomposites).<sup>60, 85, 88</sup> Other long range forces have been recognized as source of important interaction contribution (also known as non-DLVO contributions): 1) steric interactions due to adsorbed layers of polymers, surfactants or polyelectrolytes; 2) magnetic forces especially important on Fe-based NM; and 3) hydration forces come into play in structures that have bounded water (biomolecules, hydrophilic material or functional groups) and generates a repulsive interaction.<sup>89</sup>

DLVO forces act only until the primary minimum has been reached. Further fate of aggregated or deposited particles depends on the interaction at short range and then chemical specificity plays a big role. The usefulness of DLVO theory is that vdW-Ld and EDL forces are long-ranged and asymptotical. Then DLVO works fine until the energy barrier even if no good experimental or theoretical basis predicts this potential accurately up to contact between surfaces.<sup>90</sup>

However, short-range non-DLVO interactions play an important role in the case of break-up of aggregates or detachment of deposited particles. At short range the phenomena that can come in play are:<sup>90</sup>

- Electrostatic interactions that generate attractions by correlations. Briefly, if the interaction between ions is strong then there will be correlation between them and the attractive ion correlation force will be significant.
- Density variations that can generate attractive and oscillatory forces which can be due to molecular packing, capillary phase separation, and depletion due to non-adsorbing solute. Additionally, adsorption of a charged surfactant normally leads to the formation of a charged surface that generates EDL repulsion, as mentioned previously. However, if a surfactant adsorbs on an oppositely charged surface, it can make the surface electrically neutral and hydrophobic. Conversely, adsorption of a non-ionic surfactant makes a hydrophobic surface more polar, and the force between two such surfaces typically shows short range repulsion. Polymers adsorbed can induce attraction or repulsion depending on the balance between the polymer-polymer and polymer-solvent interactions.<sup>90</sup>
- Surface roughness or inhomogeneity that can generate a phenomenon called “steric energetic effect” preventing to reach full VdW adhesion energy (e.g. polished surfaces adhere easily).

### **3.3. Effects of NOM on colloidal stability**

It is possible to include the steric or entropic contribution to the repulsion potential in DLVO theory. Some models have been formulated and investigated for this purpose, for example by including empirical parameters in the attachment efficiency or including an extra DLVO parameter for accounting for the steric contribution.<sup>78, 91</sup>

NOM can be considered as a soft nanoparticulate that is present in almost all natural systems. Aquatic NOM consists of both refractory residual macromolecules from microbial degradation (humic substances), and also fresh exudates from microalgae (mainly acidic polysaccharides).<sup>92-94</sup> These different classes of NOM have been shown to have very different properties with respect to sorption and to colloidal stabilization or flocculation behavior.<sup>79, 95, 96</sup> Mosley, et al.<sup>70</sup> showed that interparticle forces for iron oxide and alumina coated with Suwannee river humic acid (SRHA) were dominated by electrostatic repulsion at low ionic strength arising from negative functional groups on the NOM. However, at very small separations (<10 nm) steric forces

from the NOM molecules were also present. Contrastingly, steric repulsion forces dominated and adhesive bridging between surfaces by adsorbed NOM was observed at high ionic strength where the electrostatic repulsion is reduced or at low pH where the SRHA is protonated. Bridging flocculation between SRHA- and alginate-coated surfaces in the presence of  $\text{Ca}^{2+}$  has also been reported,<sup>97-100</sup> suggesting that these two aquatic components are highly influential in the final fate of ENP in the environment. These observations are consistent with the results obtained in Paper VII for  $\text{TiO}_2$  and NOM.

### 3.4. Collisions between particles

Particles in aquatic media move randomly according to their Brownian motion. In the eventuality of a collision with other particles aggregation can occur. Under the assumption of neglected three body collisions (diluted conditions), the number of collisions is a second order reaction rate:

$$J_{ij} = k_{ij} \cdot n_i \cdot n_j \quad 26$$

Where  $k_{ij}$  is a second-order collision rate constant and  $n_i$  and  $n_j$  is the number concentration of particles of the class size  $i$  and  $j$  respectively;  $k_{ij}$  is referred as a cluster kernel when the integro-differential equation for population balances is used as a model for aggregation<sup>101</sup>.

In the presence of energy barriers, not all collisions will lead to attachment and the aggregation will be reaction limited (RL). An extra term is introduced to account for this: the collision efficiency,  $\alpha$ . If attractive or repulsive forces are neglected then every collision will lead to a successful attachment and this is called the diffusion limited colloid aggregation, DL. Under DL and assuming irreversibility in the attachment the following expression can be written for the variation in concentration of the  $k$ -fold aggregate:

$$\frac{dn_k}{dt} = \frac{1}{2} \sum_{\substack{i+j \rightarrow k \\ i=1}}^{i=k-1} k_{ij} \cdot n_i \cdot n_j - n_k \sum_{k=1}^{\infty} k_{ik} \cdot n_i \quad 27$$

The theoretical rate constant of aggregation of two dissimilar particles due to perikinetic collisions can be evaluated as:<sup>40</sup>

$$k_{ij} = 4 \cdot \pi \cdot R_{ij} \cdot D_{ij} \quad 28$$

with  $D_{ij}$  the mutual diffusion coefficient of particles  $i$  and  $j$  that takes the form  $(D_i+D_j)$  if the viscous drag is ignored<sup>102</sup> (it can be included empirically in the collision efficiency);  $R_{ij}$  is the collision radius which can be approximated to  $(d_{vi}+d_{vj})/2$  for spheres.

A very simple solution of the irreversible population balance equation 27 can be found to evaluate the aggregation dynamic of a destabilized colloidal suspension assuming that the particles are spherical, monodisperse and that only dimers would be formed at a rate  $k_{11}$ . Then the change of total number of particles at a given time,  $t$ , is:<sup>40</sup>

$$n_T = \frac{n_0}{1 + \frac{k_{11}}{2} \cdot n_0 \cdot t} \quad 29$$

where  $k_{11}$  is the collision rate constant for duplets evaluated with equation 28, equivalent to  $1.23 \times 10^{-17} \text{ m}^3 \cdot \text{s}^{-1}$  at 25 C.  $n_0$  is the initial number of particles. It follows that the half-life time of the reaction is:

$$t_{1/2} = \frac{2}{k_{11} \cdot n_0} \quad 30$$

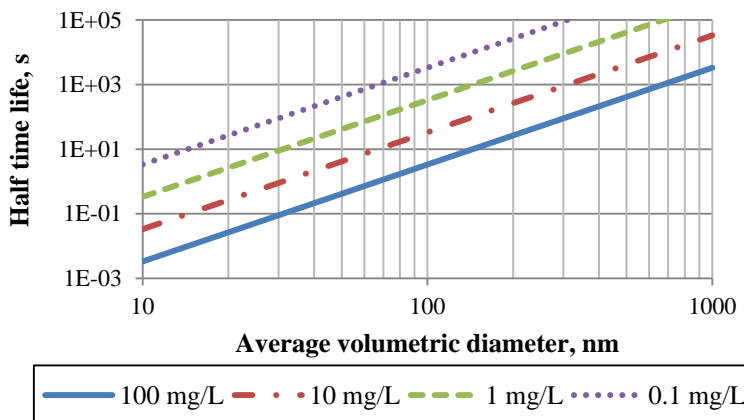
This value is also called the characteristic time. The initial particle number concentration can be calculated combining equations 10 and 11:

$$n_0 = \frac{C_0}{\rho \cdot \frac{\pi}{6} \cdot d_v^3} \quad 31$$

where  $C_0$  is the initial mass concentration of particles  $\rho$  is the density of the particles and  $d_v$  is the number-averaged volumetric diameter.

### *Expected aggregation rates for titania NP*

From the equations mentioned above it is possible to determine the time required to get the number concentration halved depending on the initial mass concentration of particles. This is presented in Figure 7 for monodisperse titania particles used in Paper VII at different starting number-averaged volumetric diameters and mass concentrations.



**Figure 7. Half-life time of monodisperse titania NP undergoing fast aggregation as a function of size for different starting concentrations.**

This half-life time indicates that once this time has passed the total number concentration will have been reduced to half the initial value. This will happen mostly by formation of duplets but there will also be formation of triplets and quadruplets. Assuming that all primary particles have disappeared to form duplets during that characteristic time, the duplet formation could be followed in different consecutive characteristic times and, in this way, an approximate value of the number-averaged diameter can be found with equation 7 assuming a  $k_f$  of 1 and a fractal dimension,  $D_f$ , according to typical values.

Usually, fast aggregation (DL) results in aggregates with fractal dimension of 1.8 (open structures) and slow aggregation (RL) results in values near 2.1 (compact structures).<sup>103</sup> Both values were evaluated for the particles used in Paper VII and the results can be found in Table 3 (20nm initial diameter titania at a concentration of 100 mg/L ( $6.11 \times 10^{18}$  part/m<sup>3</sup>) and a temperature of 25C). In this case aggregation occurs very fast because the initial concentration is relatively high. In less than one

minute aggregates approaching  $1 \mu\text{m}$  are achieved. This has implications for the measurements of aggregation rates since many techniques require measurement times that can be larger than the characteristic time of reaction in order to obtain meaningful results.

The expected behavior during this type of batch aggregation process differs slightly from the one depicted in Table 3. First of all, not all primary particles will collide to form duplets during the first characteristic time (especially in diluted systems). Many primary particles remain unreacted and the polydispersity increases. As larger particles become more abundant they will have slightly higher aggregation rates with the smaller ones (going from  $O[-17]$  for  $k_{1-1}$  to  $O[-16]$  for  $k_{1-10}$  and  $O[-14]$  for  $k_{1-1000}$ ) favoring collision of these with the remaining smaller ones that are predominant at least at the earlier time. Eventually, the concentrations drop and the collisions are more scarce leading to a semi-stable particle size distribution that in some cases can have a bimodal distribution, with a population towards the smaller particles (which did not react) and a population of larger ones that were favored during the earliest stages of the reaction.

**Table 3. Simplified evolution of average hydrodynamic diameter and total particle number concentration for 100 mg/L TiO<sub>2</sub> NP at different levels of duplet formation.**

$t_{1/2}$ , seconds	Elapsed time, seconds	i	$d_i$ , nm (Df 1.8)	$d_i$ , nm (Df 2.1)	$1 \times 10^6$ part/mL
0.03	0.03	2	29.4	27.8	305.52
0.05	0.08	4	43.2	38.7	152.76
0.11	0.19	8	63.5	53.8	76.38
0.21	0.40	16	93.3	74.9	38.19
0.43	0.82	32	137.2	104.2	19.09
0.85	1.68	64	201.6	144.9	9.55
1.70	3.38	128	296.3	201.6	4.77
3.41	6.79	256	435.5	280.4	2.39
6.81	13.60	512	640.0	390.1	1.19
13.62	27.22	1024	940.6	542.6	0.60
27.25	54.47	2048	1,382.5	754.8	0.30



The results obtained with this simplified method are not meant to be precise because of the reasons explained above. They are rather meant to give an idea of the expected size within a given time frame for this particular system consisting of an intense pulse feeding. An overall underestimation of particle sizes in the first stages of aggregation is expected due to the underestimation of aggregation rates for dissimilar particles as they are created. In contrast, at larger times the diameters predicted are larger than those measured experimentally. An appropriate population balance should be used to estimate the size evolution more precisely.<sup>101, 104, 105</sup>

### ***Aggregation rate constants for other mechanisms of collision***

The aggregation rate constant can be modified to include three types of collision mechanisms: 1) perikinetic collisions occurring because of Brownian motion. This is the most relevant mechanism for very small particles and was studied in the previous section; 2) orthokinetic collisions originating from shear stress and velocity gradients and 3) collision by differential settling.

The collision rate constant for spheres can be calculated as:<sup>29</sup>

$$K_{i,j} = \frac{2k_B T}{3\mu} \frac{(a_i + a_j)^2}{a_i a_j} + \frac{4}{3} G (a_i + a_j)^3 + \left( \frac{2\pi g}{9\mu} \right) (\rho_p - \rho_w) (a_i + a_j)^3 (a_i - a_j) \quad 32$$

where  $a_i$  and  $a_j$  are the radii of particles  $i$  and  $j$  respectively,  $G$  is the shear rate, and  $\rho_p$  and  $\rho_w$  are the densities of the particles and water, respectively.

## **3.5. Sedimentation**

The sedimentation of small particles can be formulated in terms of a control volume from which particles are lost owing to sedimentation and particles are gained from diffusion upwards (if the upper limit is considered closed, e.g. air interface). The corresponding mass conservation equation is:

$$\frac{\delta C}{\delta t} = D \cdot \frac{\delta^2 C}{\delta t^2} - v_s \cdot \frac{\delta C}{\delta x} \quad 33$$

where  $x$  is the distance in the direction of the gravity field. Equation 33 is known as the Mason-Weaver equation and has a number of analytical solutions available.<sup>106-108</sup>  $v_s$  is the Stokes (terminal) velocity:

$$v_s = \left(1 - \rho_f / \rho_p\right) \cdot g \cdot m / f \quad 34$$

Where  $\rho_p$  and  $\rho_f$  are the particle and fluid density, respectively, and  $g$  is the standard acceleration of gravity (9.81 m/s<sup>2</sup>),  $m$  is the mass of the particle (for spheres  $m = \rho_p \cdot d_v^3 \cdot \pi / 6$  with  $d_v$  the volumetric diameter) and  $f$  is the friction coefficient which, at small Reynolds number, can be expressed as a function of the hydrodynamic diameter  $f = 3 \cdot \pi \cdot \mu \cdot d_H$ . Replacing the values for equivalent spheres in equation 1,

$$v_s = \frac{(\rho_p - \rho_f) \cdot g \cdot d_v^3}{18 \cdot \mu} / d_H \quad 35$$

The last term corresponds to the Stokes diameter squared,  $d_s^2$ . For the idealized case of spheres without any coating  $d_v = d_H = d_s$ . In some cases it is necessary to correct the sedimentation velocity to account for fluctuations due to long-range hydrodynamic interactions, especially for high volume fractions of particles,  $\phi$ ,<sup>109</sup> or for slip factor for large or dense particles. However, expected aquatic environmental concentrations of NP (ENP plus NNP) are not very high to apply corrections for hydrodynamic interactions (perhaps in proximity of walls it is necessary) and the expected aggregates are relatively light to apply slip factor corrections. However, electrophoretic retardation should be revised carefully as NP in aquatic environment tend to have a charge (either coming from the surface charge or the coating) and it will generate an electrical field as they transport causing an electrophoretic force in the opposite direction of the movement.<sup>64</sup>

A practical way to evaluate if the settling motions dominate those due to Brownian diffusion is calculating Péclet numbers ( $Pe$ ) evaluated at a length equal to the hydrodynamic diameter. If  $Pe \gg 1$  then sedimentation is more important to determine the particle fate while for  $Pe \ll 1$  thermal fluctuations dominate.

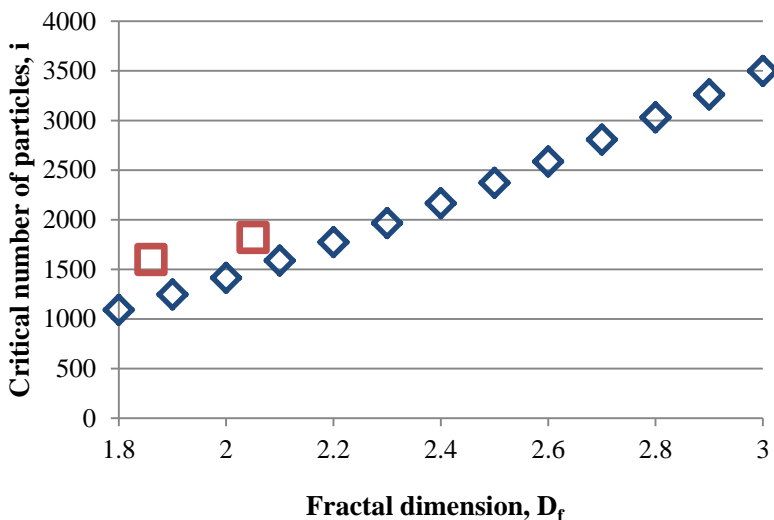
$$Pe = \frac{v_s \cdot d_H}{D} = \frac{\pi \cdot d_H \cdot d_v^3 \cdot (\rho_p - \rho_f) \cdot g}{6 \cdot k_B \cdot T} \quad 36$$

The hydrodynamic and volumetric diameters have been separated in order to maintain a general equation useful for non-spherical particles as it is the case for illite (from Paper V and Paper VI) and for fractal aggregates (Paper VI).

### ***Evaluating sedimentation for aggregates***

Aggregates of colloidal particles usually have a fractal structure that was defined in equation.7 As mentioned before, fast aggregation (DL) presents values of hydrodynamic fractal dimension of 1.8 and slow aggregation (RL) of 2.1.<sup>103</sup> In Paper VI, the critical number of 30nm Au NP necessary to reach a  $Pe$  equal 1 were evaluated assuming  $k_f=1$  for the hydrodynamic diameter of the cluster and varying fractal dimensions between 1.8 and 3. The results can be found for a temperature of 20C in Figure 8.

Figure 8 shows that, at lower fractal dimensions (i.e. faster aggregation rate) less particles are needed to generate aggregates that are more prone to settle. This implies that intermediate aggregation rates might result in more compact aggregates that are removed more rapidly compared to non-compact aggregates. This has very important implications for the fate of ENP and the final aggregation state in aquatic environment.



**Figure 8. Critical number of particles in a fractal cluster required for achieving  $Pe$  numbers of 1 as a function of fractal dimension for Au NP 30 nm. For  $Pe \gg 1$  sedimentation is dominant over diffusion. Diamonds correspond to the case where hydrodynamic diameter is calculated with  $k_f=1$  and squares correspond to values obtained by Lattuada, et al.<sup>68</sup>:  $k_f=2.37$  for  $D_f=1.86$  and  $k_f=1.81$  for  $D_f=2.05$ . Adapted from Paper VI.**

The aggregates structure for the clay particles used in Paper VI is more complex to predict since the plates can agglomerate either face-face or face-edge and this behavior is highly dependent on the pH of the solution. The clay faces bear a permanent charge due to isomorphous substitution while the edges are charged due to proton dissociation of the aluminum oxide which is pH dependent. More highly charged 2:1 clay minerals like illite are more likely to stack in order due to increased electrostatic attractions between the layers mediated by the interlayer cations. The stacking of illite particles is more likely to happen in a face-face mode forming thicker and larger spheroids and at the same time reducing the aspect ratio as more compact structures are being generated.<sup>110</sup> It has also been reported that aggregates of illite particles will have fractal dimensions above the suggested values for spheres.<sup>111</sup>

### 3.6. Large scale models

The population balance models are based on colloid stability theory and particle collision theory and algorithms for sedimentation rate.<sup>29</sup> The

colloid stability and aggregation processes can either be modelled from the DLVO theory<sup>40</sup> or derived from experimental data. The collision theory formulated by Arvidsson, et al.<sup>29</sup> is based on the early works by Smoluchowski,<sup>41</sup> Friedlander<sup>112</sup> and Grant et al.<sup>113</sup> The governing equation for this model is:

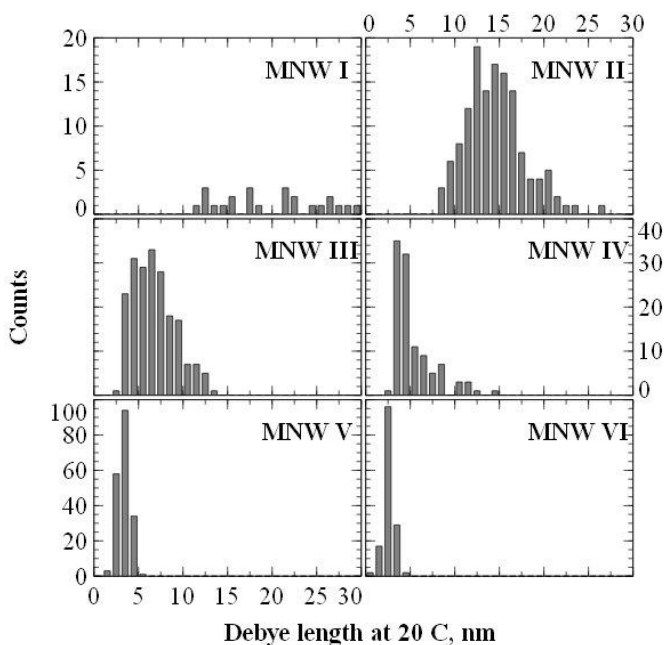
$$\frac{dn_j}{dt} = \frac{1}{2} \sum_{i=1}^{j-1} \alpha_{i,j-i} K_{i,j-i} n_i n_{j-i} - n_j \sum_{i=1}^{j-1} \alpha_{i,j} K_{i,j} n_i - \frac{v_s}{d} j^\beta n_j + I_j - n_j \sum_{i=1}^{i=\infty} \gamma_{i,j} H_{i,j} c_i \quad 37$$

where  $n_j$  is the particle number concentration of particle class  $j$ ,  $\alpha_{i,j}$  and  $\alpha_{i,j-i}$  are collision efficiencies,  $K_{ij}$  and  $K_{i,j-i}$  are rate constants,  $v_s$  is the sedimentation rate of primary particles,  $\beta$  is a form factor (2/3 for spherical particles),  $d$  is the depth of the water compartment,  $I_j$  is the inflow of particles,  $\gamma$  is the collision efficiency,  $H$  is the rate constant for collisions between natural colloids and synthetic nanoparticles (which in principle could be calculated in the same form as  $k_{ij}$ ), and  $c_i$  is the concentration of an agglomerate with  $i$  primary natural colloids. The first term on the right side of the equation describes the formation of particle  $j$  through agglomeration of particles  $i$  and  $j-i$ . The second term describes the loss of particle  $j$  through agglomeration with other particles  $i$ . The third term describes sedimentation, and the fourth term for the inflow of particles. The equation is based on the assumption that the particles are spherical. The effects of NOM are usually included empirically via the collision efficiency,  $\alpha$ . The effects of dissolution, breakage or flotation are not included.

## 4. ENP fate platform on a continental watershed scale

In Paper IV a geographically distributed classification of surface water chemical parameters influencing fate and behavior of nanoparticles and colloid facilitated contaminant transport was introduced. A compilation of river quality geochemical data with information about multi-element composition for near 800 rivers and streams in Europe<sup>114</sup> was used to perform a principal component analysis (PCA) and define 6 contrasting water classes (model natural waters, MNW) using 12 chemical parameters from 66 available in the database. These included pH, electric conductivity,  $\text{HCO}_3^-$ /alkalinity (alkalinity determined by titrating 100 ml of water with  $\text{H}_2\text{SO}_4$  to pH 4.5 and expressed as  $\text{HCO}_3^-$  mg/L),  $\text{Cl}^-$ ,  $\text{SO}_4^{2-}$ ,  $\text{NO}_3^-$ ,  $\text{K}^+$ ,  $\text{Na}^+$ ,  $\text{Mg}^{2+}$ ,  $\text{Ca}^{2+}$ ,  $\text{SiO}_2$  (total Si, recalculated to  $\text{SiO}_2$ ) and NPOC (non-purgeable organic carbon, filtered through 0,45  $\mu\text{m}$ , acidified and sparged; equivalent to dissolved organic carbon, DOC). EC is given in mS/m and all the other parameters in mg/L.

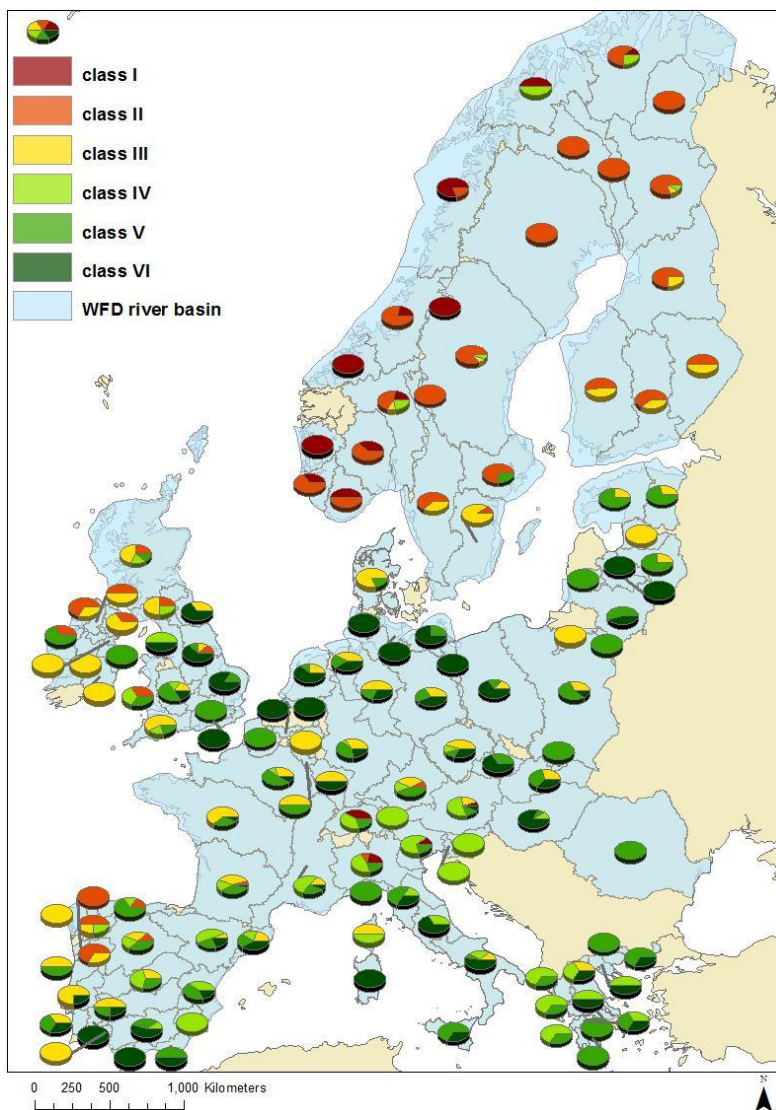
Critical factors for the stability of NP and colloids in a suspension are a combination of particle specific properties (size, shape, surface charge, Hamaker coefficients, and functionalization) and solution composition (ion concentration, affinity to the surface and valence, DOC quantity and quality, suspended solids and colloids). As it could be seen in the section 2 (equation 24), the electrostatic colloidal stability of NP in the environment is dependent on the Debye-Hückel parameter. Even for NP with a coating of NOM, it has been shown that the stability provided by the natural coating is partly due to electrostatic repulsion. For that reason in Paper IV it was decided to introduce the Debye length (which is inversely proportional to the square root of IS, see equation 13) as a preliminary indicator of the stability (or instability) of NP and colloids in river waters. The distribution of Debye length in the six MNW is presented in Figure 9.



**Figure 9. Histograms of the distribution of Debye lengths in all sample points differentiated by model natural water (MNW) class.**

With the aid of geographical information system algorithms, it was possible to analyze how the different sampling locations were predominantly represented within each European Water Framework Directive (WFD) drainage basin.<sup>115</sup> The map representing the proportion of sampling sites within each MNW in each river basin is presented in Figure 10. These water classes and their associated Debye-Hückel parameter can be considered as determining factors to evaluate the large scale fate and behavior of nanomaterials and other colloid-transported pollutants in the European aquatic environment.

The MNW presented in Paper IV can be used in fate studies in microcosms under controlled conditions to identify the final location and state of NP, with the advantage over natural surface waters, that experiments with the 6 MNW would be reproducible over a broad range of European natural river waters.



**Figure 10. Geographical distribution of the different water classes in major European river-basin districts. Areas that are not covered are either not covered by the River basin districts database or no sampling points fall into the specific district. The classes are colored according to IS with red representing the lowest IS (MNW I) and dark green the highest IS (MNW VI). The chart pies show the percentage of each class in the respective WFD river basin district. Adapted from Paper IV with permission. Hammes et al <sup>25</sup>, copyrights ELSEVIER 2013.**



The composition suggested for the MNW is presented in Table 4. Suwannee River NOM is suggested to be used as a source of NOM in order to increase reproducibility between different experiments. However, it has been demonstrated in this study and by others that different qualities of NOM can have very distinct effects on the stability and transformation of ENP.

**Table 4. Composition of the model natural waters (MNW) generated in Paper IV. Ionic strength and ion composition in mM. Adapted with permission. Hammes et al <sup>25</sup>, copyrights ELSEVIER 2013.**

Parameters	I	II	III	IV	V	VI
pH	7.01	6.2	7.29	8.15	8.01	8.02
Ionic strength	0.247	0.430	2.60	3.16	6.47	16.5
HCO <sub>3</sub> <sup>-</sup>	0.076	0.186	0.732	0.515	1.237	3.260
Cl <sup>-</sup>	0.026	0.106	0.527	0.166	0.716	5.121
NO <sub>3</sub> <sup>-</sup>	0.002	0.009	0.197	0.072	0.330	0.478
K <sup>+</sup>	0.007	0.015	0.085	0.029	0.086	0.282
Na <sup>+</sup>	0.049	0.131	0.557	0.228	0.696	2.977
Mg <sup>2+</sup>	0.017	0.033	0.179	0.180	0.380	1.917
Ca <sup>2+</sup>	0.044	0.094	0.507	0.549	1.512	2.845
SO <sub>4</sub> <sup>2-</sup>	0.022	0.018	0.227	0.347	0.901	1.894
DOC, mg/L	1.84	12.48	11.05	1.75	4.6	8.63

These MNW were used in the microcosms in Paper VI for the assessment of heteroaggregation and sedimentation under quiescent conditions of citrate-coated Au NP with illite particles. This methodology for the identification of geographically distributed surface water chemical parameters can be extended to different regions in larger or smaller scale. Furthermore, the Debye length combined with microcosm experiments can be used as an input for mathematical models in order to predict environmental fate and transport of NP and colloids. The Debye length, pH, NOM content and quality and colloidal concentrations in a water body could likely be utilized as early indicator of potential NP and colloids stability and mobility.



## 5. Fate processes

Fate processes in ENP risk assessment here refers to the transport, transformation and accumulation in the environment. For ENP several transformations processes were identified in Paper III and those relevant for water environment are listed below:

- Photochemical transformations either by generation of free radicals,<sup>116</sup> by direct interaction with other components of the ENP<sup>117</sup> or dynamically interfering with the interaction of ENP with environmental components.
- Redox reactions can occur if the reaction is thermodynamically favorable and the reactants can reach the surface of the ENP (i.e. diffusion limitations).
- Dissolution or the production of individual ions or molecules that are soluble in water.<sup>118, 119</sup> The dissolution process can involve reaction of the surface molecules and ultimate release of the ionic form<sup>120</sup> or direct dissolution of the constituent materials, followed by diffusional transport of the dissolved compounds.<sup>121</sup> Dissolution has been recognized as an important processes in the aquatic fate of Ag NP in oxidizing environments<sup>120</sup> and for ZnO NP.
- Re-precipitation is the formation of new solid phase after dissolution has taken place. It can be a solid heavy enough to precipitate or a new suspended colloid or NP. The formation of these particulate materials adds another level of complexity to the evaluation of fate of the original ENP. The formation of Ag<sub>2</sub>S in WWTP is a renowned case in this category.<sup>122-124</sup>
- Adsorption / desorption the process by which substances attach to the surface of solids by means of Van der Waals attractions (i.e. physisorption), electrostatic interactions (i.e. ion exchange) or chemical bonding (i.e. chemisorption). The sorption of NOM is considered one of the most relevant cases for environmental transformation and this can lead to further stabilization or coagulation of ENP. Sorption of contaminants to nanomaterials is considered an important process that can lead to enhanced transport or changed bioavailability of the contaminant.<sup>22, 25</sup> Significant desorption of adsorbed substances will occur only if

the equilibrium with the medium is altered and the dissociation kinetics are not too slow.

- Biotransformation or biodegradation may induce transformation of the ENP<sup>125</sup> or the transformation product.<sup>126</sup>
- Physical forces (e.g. turbulent fluid regimes or strong collision of solid materials) can induce the breakdown of the original material and the release of ENP or ENM-containing particles in different shapes and sizes.<sup>127-129</sup> Shear stress can also break apart aggregates depending on the strength of the cohesive forces.<sup>130</sup>

These processes are highly related to the water chemistry, hydrodynamic conditions (number of contacts) and the presence of other interfaces (e.g. suspended solids, rocks, biofilms, and gas-water interfaces). For example, it has been observed that ENP can undergo dissolution and acquire a coating of Ag<sub>2</sub>S under certain circumstances.<sup>131</sup>

The transport and accumulation of NP includes deposition, aggregation and agglomeration (usually referred in that form for the reversible and irreversible attachment, respectively) and the advective and convective mobility. This implicates that pristine or transformed ENP mobilizes as the transformation processes occur and the extent to which all of these processes (transformation and transport) occur will be defined by the relative extent of their characteristic times; they are parallel processes and they depend on each other.

In the sections below a set of experimental and theoretical works is presented which contains the main finding on the investigations of some of these transformation and transportation processes.

## 5.1. Aggregation and agglomeration

Aggregation and agglomeration of ENP in the environment has been considered as a universal fate process that will determine the final concentrations in natural waters.<sup>132</sup> The aggregation and heteroaggregation rates of NP and colloids can be characterized by the collision efficiency,  $\alpha$ , defined in equation 25 which describes the likelihood of a collision between particles that lead to a permanent attachment.<sup>29</sup> When the collision efficiencies are 1 the system is

completely destabilized and the limiting factor in the aggregation is the number of collisions (diffusion limited).

One of the most common ways to estimate attachments efficiencies is by using time-resolved dynamic light scattering, TR-DLS.

***TR-DLS collision efficiency.***

In Dynamic Light Scattering, DLS technique, the intensity of the scattered light by an ensemble of particles is measured at a given angle as a function of time. The Brownian motion of the dispersed particles determines the rate of change of the scattered light intensity.<sup>61</sup> Autocorrelation functions of the fluctuations in scattered light are obtained and the exponential decay of the first order autocorrelation function is related to the ensemble-averaged diffusion coefficient. The Cumulants analysis<sup>133</sup> uses the initial part of the exponential decay curve of the autocorrelation function to determine the intensity-weighted average hydrodynamic-diameter. The diameter obtained by this method is usually called zeta-average diameter.

A fixed concentration of NP is thoroughly mixed with the media containing electrolytes and other constituents and the rate of increase of the zeta-average hydrodynamic diameter is measured. If the initial number concentrations are kept constant and at low levels so that the aggregation times of the most unstable conditions can be followed, then the collision efficiency can be calculated as the ratio between the slopes obtained at a given concentration versus the maximum slope (diffusion limited):<sup>134</sup>

$$\alpha = \frac{\left[ \frac{d(d_H)}{dt} \right]_{t \rightarrow 0}}{\left[ \frac{d(d_H)}{dt} \right]_{max, t \rightarrow 0}} \quad 38$$

Where  $\alpha$  is the collision efficiency and  $d_H$  is the hydrodynamic diameter. Since the hydrodynamic diameter is a zeta-averaged value that is biased towards larger sizes then the value for the collision efficiency is also a zeta averaged value. Nevertheless, this method provides a good indicator for the tendency of the particles to aggregate in the media tested.

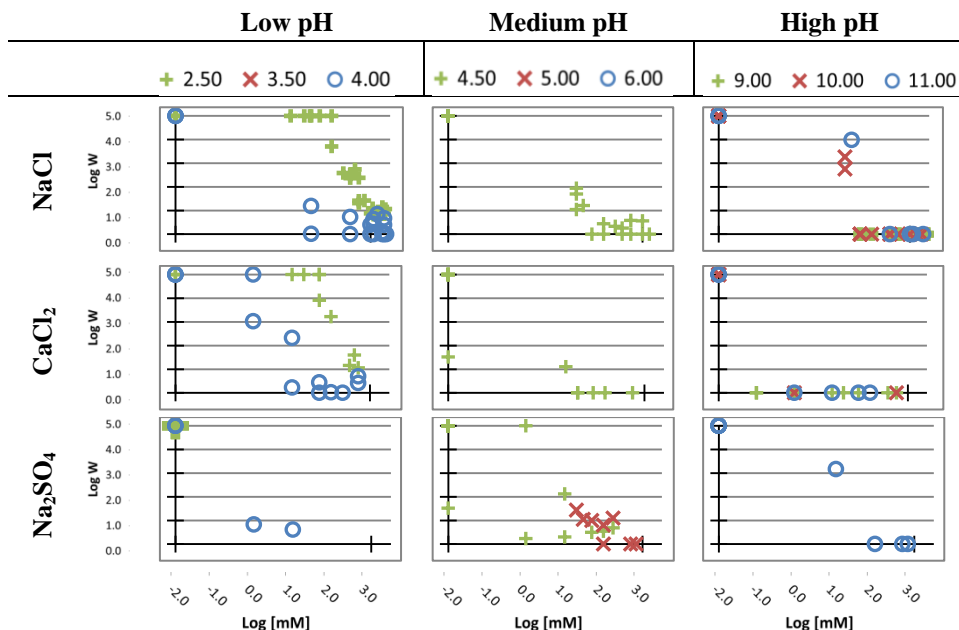
In Paper VI equation 40 was used to evaluate the aggregation rates of Au NP in model natural waters containing illite particles. The concentrations of Au were 1 order of magnitude higher than illite and NOM and therefore the illite signal was mitigated. In order to compare the aggregation rates in natural waters, the aggregation of Au NP in NaCl was evaluated and the maximum rate was used as the denominator for these zeta-collision efficiencies.

In Paper VII the aggregation rates of TiO<sub>2</sub> NP were measured using a more complete analysis in order to counteract the effects of higher aggregation rates since the particle number concentrations required for detection were 2 orders of magnitude higher than the ones used for Au in Paper VI. The approach was to follow the original derivations of Borkovec et al.<sup>134</sup> and combining variations in zeta-averaged hydrodynamic diameters and intensity scattered provided by the instrument (Zetasizer Nano ZS, Malvern instruments, UK). The final result expressed for the stability ratio,  $W=I/\alpha$ , is:

$$W = \frac{\frac{8 \cdot k_B \cdot T}{3 \cdot \mu} \cdot \left( \frac{(R_{ha} + R_{h1})^2}{4 \cdot R_{ha} \cdot R_{h1}} \right)}{\frac{1}{N_0} \cdot \left( \left( \frac{1}{R_h(0)} \cdot \left. \frac{d(R_h(t))}{dt} \right|_{t \rightarrow 0} \right) \cdot \left( \frac{R_{h2} - R_{h1}}{R_{h2}} \right)^{-1} - \left( \frac{1}{I_{h0}} \cdot \left. \frac{d(I(t))}{dt} \right|_{t \rightarrow 0} \right) \right)} \quad 39$$

where  $N_0$  is the initial particle number concentration,  $R_h(t)$  is the hydrodynamic radius evaluated at time  $t$ , the expression  $(R_{h2}-R_{h1})/R_{h2}$  corresponds to the relative change between the primary particle and the duplet.  $I$  is the scattering intensity which was obtained from the mean photon count rate.

Results obtained for NaCl, Na<sub>2</sub>SO<sub>4</sub> and CaCl<sub>2</sub> at varying values of pH range are presented in Figure 11.



**Figure 11. Variations in stability ratio,  $W$ , at different values of pH (symbols) and pH range (columns).**

In general, all additions of electrolytes without NOM followed the DLVO theory and the order of magnitude of the calculated stability ratios (Figure 6). Positively charged NP at low pH were more prone to destabilization by  $\text{SO}_4^{-2}$  compared to  $\text{Cl}^-$  and the opposite holds for  $\text{Ca}^{+2}$  compared to  $\text{Na}^+$  at high pH. If the pH of the suspension is away from the IEP (in this case around pH 6) the particles have a higher charge (either positive or negative) and this leads to slower aggregation rates at similar electrolyte concentration than particles closer to IEP.

## 5.2. NOM-sorption: effects on stability

In Paper VII it was shown that at sufficient NOM/ $\text{TiO}_2$  ratios (i.e. molar ratio HA/ $\text{TiO}_2$  above 283), adsorption of NOM on the surface provided a negative net surface charge of the suspended particles and particles aggregates. In the same paper, the stability ratios of  $\text{TiO}_2$  were calculated after different additions of biopolymeric (sodium alginate) and refractory macromolecules (humic and fulvic acids); all the macromolecules were added in excess of the NOM/ $\text{TiO}_2$  stability ratio. The results are resumed below:

- The addition of NOM-stabilized suspensions presented increased stability of the systems with respect to NaCl and Na<sub>2</sub>SO<sub>4</sub>.
- Ca<sup>2+</sup> presented indications of bridging coagulation between the organic molecules. Calcium is known to bridge the molecules in the alginate network ( $\beta$ -D-mannuronate and  $\alpha$ -L-guluronate) to form gel like aggregates. Particles with HA have also shown low stability in the presence of calcium.<sup>135</sup> Other studies with silica particles (150 nm z-average) have shown that Ca<sup>2+</sup> ions destabilize the suspension in the presence of alginate and humic acid but not with fulvic acid.<sup>136</sup>
- The presence of NOM increased the stability in the presence of Na<sub>2</sub>SO<sub>4</sub> in a more efficient way than for the other 2 electrolytes.
- HA was less effective in stabilizing NP at low pH. HA is, by definition, not stable in suspension at pH below 2 and, therefore, at low pH the overall surface charge were low and there was reduced electrostatic contribution to the repulsion.
- FA was better stabilizer even at low pH probably because FA possesses more charge at low pH than HA leading to an improved electrostatic stabilization.

Given the considerations presented above, it is important to highlight that the surface coverage of NP with NOM will be highly dependent on the ratio between the number of NP and natural macromolecules (or available surface area more precisely). Therefore, it is more appropriate to speak in terms of environmentally relevant concentration-ratios instead of speaking of environmentally relevant concentrations only. Unfortunately, it has to be recognized that the number of scenarios which have environmentally relevant NOM/ENP ratios can be large and difficult to test and predict because of the great variability of NOM concentrations and quality in different aquatic environments (not to mention the presence of natural aquatic colloids) and the uncertainty regarding the expected concentrations of ENP (Paper III).

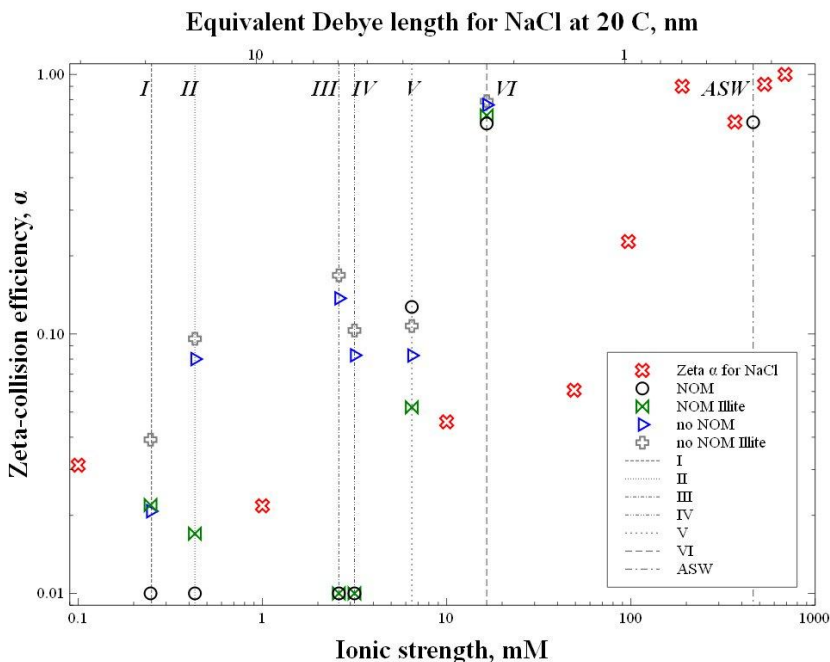
### 5.3. Sedimentation

In Paper VI on the fate of 30 nm citrate-coated Au nanoparticles (NP) was evaluated using the six MNW developed in Paper IV. Model natural freshwater covering the range of European water chemistry and artificial seawater were used to assess the environmental fate of Au nanoparticles.



Au NP were chosen because they are easily followed by NTA and ICP-MS and it is a dense material which amplifies the effects of sedimentation allowing to perform analysis in shorter times than for other materials. The evaluation of heteroaggregation and sedimentation behavior was performed with the addition of the clay mineral illite as a model natural colloid which is often present in freshwater environments.<sup>137, 138</sup>

TR-DLS was used to determine the aggregation rates of gold nanoparticles in separate batch tests at a concentration of 10 mg/L and compared with the maximum aggregation rate obtained with NaCl to determine zeta-averaged collision efficiencies (equation 38). The obtained results are presented in Figure 12.



**Figure 12. Zeta-collision efficiencies calculated for AuNP. Values below 0.01 are presented as 0.01. The upper x-axis corresponds to the Debye-length calculated as a function of ionic strength. Vertical dotted lines correspond to the composition of the different water chemistries and are drawn as a guide.**

The concentrations of Au used in TR-DLS were much higher than those of illite in order to achieve good signal intensities for the measurement

with DLS and, therefore, Au dominates the scattering intensity and the rates of aggregation reflect mostly the aggregation of gold. In MNW I to V the rates were significantly reduced in the presence of NOM indicating some increase in stability. The suspensions in MNW VI and artificial seawater (ASW)

In separate experiments low concentrations of gold nanoparticles (80  $\mu\text{g/L}$ ) were thoroughly mixed with one liter of the different MNW as receiving medium (one set containing 650  $\mu\text{g/L}$  illite as a model natural particle and the other without).

The resulting suspension was then introduced into microcosms (modified Imhoff cones) and kept at constant temperature for nearly two months under still conditions. Parallel experiments were carried out with illite only as controls. The sampling from the microcosms was done at a point located 4 cm below the surface of the water column (Figure 13).

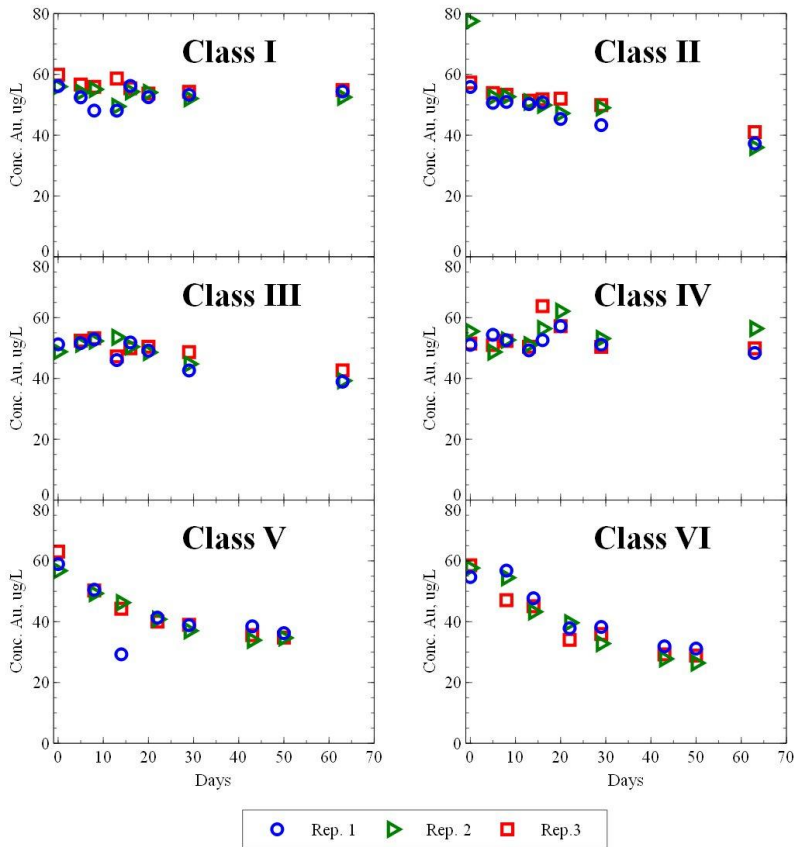


**Figure 13. Photography of the experimental setup for the evaluation of sedimentation and aggregation of ENP in MNW. Photo: Julia Hammes**

Aggregation and sedimentation were evaluated using NTA and ICP-MS measurements from samples taken at regular intervals. The results obtained for the experiments containing illite are presented in Figure 14 for ICP-MS measurements of Au. NTA measurements at the start and end of the experiments for MNW I and VI (1 replicate and control) are presented in Figure 15 and Figure 16.

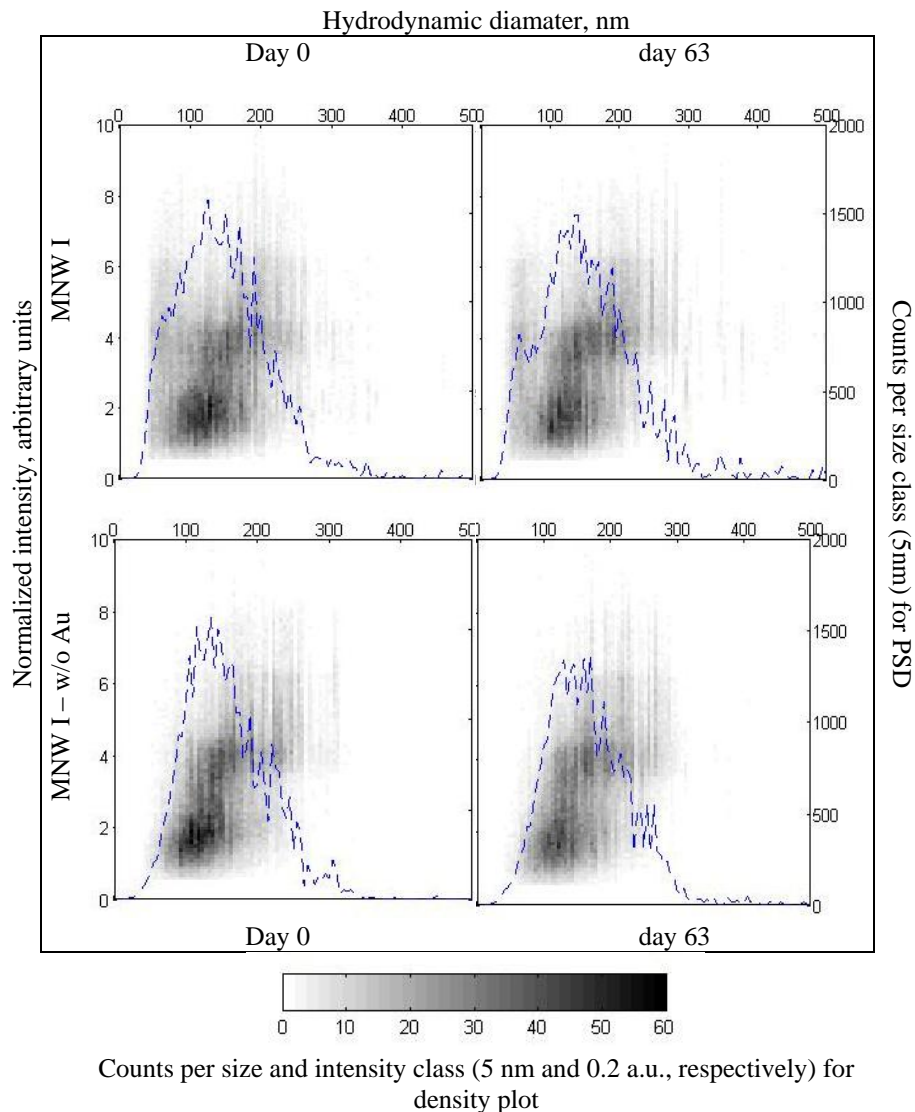
The main observation from the ICP-MS measurements is the consistent presence of elemental Au in all water classes even 2 months after the start of the experiments. MNW V and VI exhibited the maximum rates

of removal from 60  $\mu\text{g/L}$  in the first day to concentrations in the last day of 39 and 30  $\mu\text{g/L}$ , respectively.



**Figure 14. Elemental measurements of Au in the microcosms for 6 artificial natural waters during a period of 60 days using illite as a model natural colloid. Three replicates are presented for each treatment. Adapted from Paper VI.**

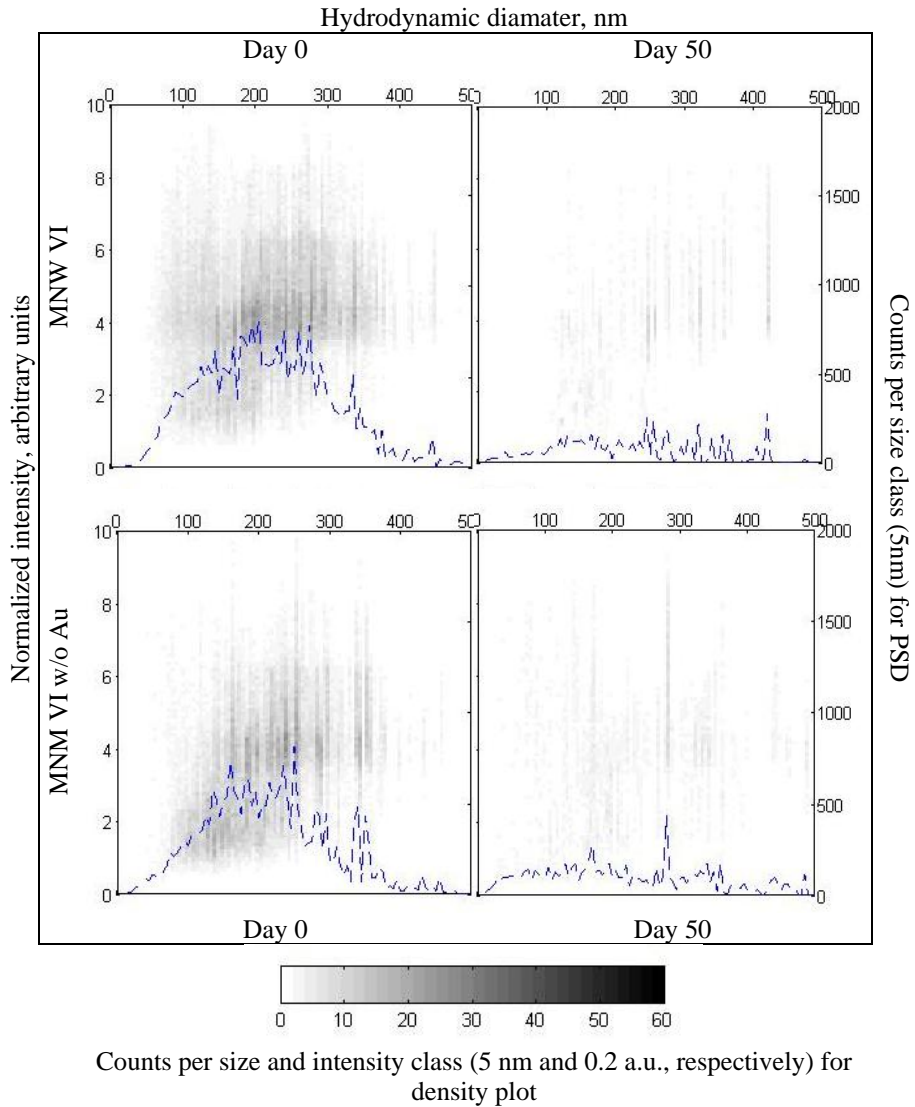
The results from NTA showed that Au NP and illite particles could be detected separately by using the intensity plots in Figure 15 and Figure 16. The number concentrations remained stable for the length of the experiment for MNW I, II, III and IV. MNW V did not show the “intensity signal” for Au NP but illite remained in suspension.



**Figure 15. Density plots of particle size and scattered-light intensity distribution combined with PSD. Au NP and illite particles in MNW I measured with NTA. Upper and lower panels present the results with and without Au, respectively. The PSD is presented for more clarity on the amount of particles corresponding to each intensity. Adapted from Paper VI.**

MNW VI showed a large reduction of the particle number concentration (both illite and Au NP) even from the start of the experiment and the

PSD showed that the smaller particles were significantly less than for the other treatments.



**Figure 16. Density plots of particle size and scattered-light intensity distribution combined with PSD. Au NP and illite particles in MNW VI measured with NTA. Upper and lower panels present the results with and without Au, respectively. The PSD is presented for more clarity on the amount of particles corresponding to each intensity. Adapted from Paper VI.**

While some aggregation was observed, mostly consistent with the IS, the sedimentation of gold nanoparticles appeared limited in all water classes, regardless of the presence of illite as shown by the elemental gold measurements. The Debye-Hückel parameters of the different water classes appeared to be determining factors to evaluate the large-scale fate and behavior of NP and other colloid-transported pollutants in the MNW containing illite particles.

In principle, it could be possible to fit rates of sedimentation to total mass loss<sup>44</sup> in Figure 14 but doing so would cover the effects of the different fate processes highlighted in the theory section. There is concomitant aggregation plus sedimentation and both are summed to create an overall mass loss. The relative contribution of these differs depending on the water composition.

For example, MNW V presented a decline of elemental Au from the water column from the first day and reached a final semi-stable concentration of about 39  $\mu\text{g/L}$ ; contrastingly, MNW VI had an initial plateau the first days and then decayed at a faster rate than MNW V and reached a semi-stable mass concentration around 30  $\mu\text{g/L}$ . According to NTA measurements, there was illite left in the suspension with MNW V after 50 days (see Paper VI) while in MNW VI illite and gold settled out of the water column.

One possible explanation for that phenomenon is that illite remained relatively stable in suspension in MNW V (no interactions with Au or other illite particles) while Au NP were less stable and aggregated to form compact and heavier aggregates which settled faster but the process was self-inhibited as the number of particles decreased. This would be in accordance to the theory of fractal aggregation for RL conditions (i.e. slow aggregation produces more compact aggregates, Figure 8). Conversely, in MNW VI both illite and Au were unstable which could have led to 1) more open structures of Au NP aggregates and 2) heteroaggregates of Au and illite, both of which have less effective density than a compact aggregate of Au NP. Therefore, these aggregated particles, differently from the ones in MNW V were less prone to settle but instead continued the process of aggregation for longer times collecting more Au NP until they became heavier and settled out leaving in this form less particles. The effects of possible differential

sedimentation flocculation can also be more important for these larger structures.

This case exemplifies the complexity involved in the exposure assessment of ENP in aquatic environments. It appears thus promising to try to fit kinetic models like those presented in the theory section to results obtained in experimental tests for fate of ENP in model natural waters.

However, ENP fate in real aquatic systems are even more challenging to predict due to the presence of other parameters like velocity gradients that are always present in natural rivers, different types of NOM, larger solids carried by the turbulent streams and the presence of microorganisms.

## 6. Concluding remarks and future perspectives

The environmental risk assessment of materials derived from the use of nanotechnology requires a thorough understanding of the physicochemical aspects governing the fate processes which ultimately will lead to exposure of organisms and determine the environmental concentrations. A theoretical framework in connection with the physicochemical aspects of NP in aquatic environments was presented. These physicochemical characteristics were then coupled to the different fate and transport processes that can influence the environmental concentrations of ENP.

Paper I provided the initial assessment of the dynamic aspects of NP in aquatic media. With help of a novel analytical technique, NTA, it was shown that NNP are ubiquitous in the environment and approximate number concentrations and PSD were provided. Paper II introduced the applicability of NTA for measuring NP in natural samples and ecotoxicological tests and provided some insight into the capabilities and limitations of this technique in terms of scattering properties of the material and its dependence on hydrodynamic diameter. Further, in Paper V it was demonstrated that NTA capabilities to detect NP in water will not only depend on size and material but also on the shape of the NP, i.e. a spherical particle with a given hydrodynamic diameter will scatter light more efficiently than a high-aspect ratio particle with the same hydrodynamic diameter. It was also shown in Paper VI that NTA offers the possibility to evaluate different populations of contrasting NP using the differential scattering properties mentioned above. However, it is unclear to what extent in terms of different size this differential scattering identification can be used since the control volume, where particles can be identified and counted, is also variable and depends on the scattering properties.

The theoretical framework and the results from Paper V have served to illustrate the importance of identifying the differences in the actual shape of a particle for determining to which extent the fate processes will be



important and for correctly interpreting the results from characterization of particles using different instrumentation. It was shown that shape can influence the aggregation rate constants by means of the hydrodynamic diameter and the radius of contact, the sedimentation propensity through the Stokes diameter and the potential of interaction between surfaces by means of the structural configuration.

The quality and quantity of NOM existing in the aquatic environment will determine the stability that they can provide to ENP. Fulvic compounds, refractory organic matter and rigid biopolymers are some of the most common components of NOM<sup>51</sup> and their molecular structure will depend on the biogeochemical characteristics of the surrounding landscape. The NOM/ENP mass ratio will determine the degree of sorption and the process of mixing can lead to different states of aggregation, e.g. NOM sorption can induce small and stable aggregate formation during the mixing process if the number of collisions between particles is relatively high.

Predominantly, electrolytes and pH determine the extent of repulsion by electrostatic or electro-steric mechanisms and NOM can provide some additional stabilization or cause aggregation depending on the surface coverage of the particles. The effects of these parameters on the stability of titania nanoparticles were studied in Paper VII with three types of macromolecules and three electrolytes commonly found in natural waters. Results showed that calcium aided the coagulation of particles when HA and ALG were present probably by bridging between NOM molecules. The implications of this study are that different types of NOM will have different interactions with the constituents of the water body and the ENP.

One of the most influencing parameters on nanoparticle stability is the IS and the corresponding Debye length. In those water classes presented in Paper IV that have low IS, aggregation and sedimentation rates are expected to be low and exposure of aquatic organisms to NP or small aggregates will be more likely than in waters with high IS. On the contrary, in high IS waters there will be loss of NP by sedimentation but, if small concentrations of NP are present they will require longer times for generating settable aggregates and these will remain in the water column in the form of large particulate matter as it was shown in Paper

VI. This could have implications in contaminant transport and transitory release of ions as the aggregates dissolve and redistribute. The effects of other hydrodynamic conditions different than the quiescent waters tested, as well as the presence of different types and quantities of NOM and NNP may lead to different outcomes.

The aggregation rates measured in Paper VI (Figure 12) showed that high concentrations of NP are needed to obtain statistically significant hydrodynamic diameters with TR-DLS. The results obtained in these tests, even though helpful to identify trends in aggregation of ENP, might not be easily extrapolated to real aquatic environments owing to the high dependence of aggregation on the number of particles. As the aggregation process continues larger particles have a higher reaction rate with smaller particles and the aggregation will be enhanced and perhaps not directly comparable to real aquatic environments where lower concentrations are expected. The ratio between ENP, NOM and NNP will also be different and the surface coating with NOM and reactions rates with NNP will have a different effect on the overall aggregation process.

The heteroaggregation and sedimentation processes studied in Paper VI showed that aggregation of ENP can lead to different outcomes depending on the initial concentration and the chemical constituents of the water body. It was shown that different aggregation regimes will generate aggregates with a different fractal structure which in turn will be reflected in a different settling behavior. Slow aggregation will likely result in compact structures, fast aggregation will generate more open structures and heteroaggregation, in turn, will form lower density aggregates that can be open or compact. Compact structures results in a larger Stokes diameter (equation 3) leading to faster sedimentation and flocculation slows down as the number of particles diminishes leading to a larger concentration of gold remaining in the water column compared to the fast aggregation case. In the fast aggregation case, open structures may remain longer time in the water column, enhancing thus aggregation since unequal spheres have higher aggregation rate constants and sedimentation flocculation can take place. The open structures grow and settle leaving smaller aggregates in the water column which is reflected in a lower concentration of elemental gold than for the slow aggregation case.

Analytical techniques able to investigate the fate processes of NP in the environment are lacking. The dynamic nature of the processes involved require the continuous monitoring of number concentrations, PSD and elemental composition in a wide range of particle sizes that are not yet available. More sensitive methods which allow measuring dynamic behaviour for lower concentrations are in need.

The effects of hydrodynamic interactions in the fate of NP in aquatic environments are a topic that has not been fully studied. Turbulence is present in almost all natural waters to certain degree and experimental and theoretical frameworks are needed to understand the effects that mixing can have in the different fate processes.

## 7. Acknowledgements

I would like to thank and applaud the support, politeness and professionalism of my main supervisor Martin Hassellöv. It has been a privilege to work with you. Special thanks to Aldina Bijedik, Julia Hammes, Mohammad Aurangjob and Tobias Palander for all the data collected for the papers.

This would not have been possible to achieve without the constant support of Maria and my family in Colombia.

All the co-supervisors have provided extremely helpful insights into the scientific, technical and managerial aspects of the scientific labor that are greatly acknowledged. A large part of this work has been motivated by the scientific exchange with the colloidal chemistry group at the Department of Chemistry and Molecular Biology.

To all the former and current members of the “environmental nanochemistry group”, Ángela, Kajsa, Eike, Jenny, Jani, Tobias, Julia, Karin, Caroline, Geert, Zareen, Martin and visitors PhD students, I would like to express my sincere gratitude for all the help and experiences acquired. The colleagues and friends from Nanosphere are also greatly acknowledged for the academic exchange.

All the people in AMK are greatly acknowledged for all those shared moments in the lunchroom and defense parties.

The partners, colleagues and friends in different institutions and projects with whom I have had some connection are greatly acknowledged: NIVA, University of Aveiro, Nanofate, Department of Biology and Environmental Sciences.

For all the support in the administrative paperwork and technical details thanks to all the administrative and technical personal of the Department of Chemistry and Molecular Biology.

Financial support during the whole PhD was received for salary, travel support and equipment from the Swedish Research council, FORMAS,

the research platform from the University of Gothenburg "Nanopartiklar i interaktiva miljöer", the European Chemical Industry Council (CEFIC), The Nordic council of ministers (NORDEN), NanoFATE Collaborative Project CP-FP 247739 (2010-2014) under the 7th Framework Programme of the European Commission (FP7-NMP-ENV-2009, Theme 4), Wilhem och Martina Lundgrens vetenskapsfond, Adlerbertska stipendiestiftelsen, Adlerbertska hospitiestiftelsen, Stiftelsen Paul och Marie Berghaus donationsfond, Nanosphere (Center for Interaction and Risk studies in Nano-Bio-Geo-Socio-Techno-sphere interfaces) funded by FORMAS, Sweden.

Thanks for the earlier financial support to COLFUTURO which allowed me to travel abroad and learn much more than I had expected (in the academic and personal aspect).

## 8. References

1. M. C. Roco, *The long view of nanotechnology development: the National Nanotechnology Initiative at 10 years*, *J. Nanopart. Res.*, 2011, **13**, 427-445.
2. R. Vajtai, *Springer Handbook of Nanomaterials*, Springer Berlin Heidelberg, Berlin, Heidelberg, 2013.
3. P. J. J. Alvarez, V. Colvin, J. Lead and V. Stone, *Research Priorities to Advance Eco-Responsible Nanotechnology*, *ACS Nano*, 2009, **3**, 1616-1619.
4. C. J. Van Leeuwen and T. G. Vermeire, *Risk Assessment of Chemicals: An Introduction*, 2nd edn., Springer, Dordrecht, 2007.
5. M. R. Wiesner, G. V. Lowry, E. Casman, P. M. Bertsch, C. W. Matson, R. T. Di Giulio, J. Liu and M. F. Hochella, *Meditations on the Ubiquity and Mutability of Nano-Sized Materials in the Environment*, *ACS Nano*, 2011, **5**, 8466-8470.
6. M. Auffan, J. Rose, J. Y. Y. Bottero, G. V. V. Lowry, J. P. P. Jolivet and M. R. R. Wiesner, *Towards a definition of inorganic nanoparticles from an environmental, health and safety perspective*, *Nat. Nanotechnol.*, 2009, **4**, 634-641.
7. M. Auffan, E. Flahaut, A. Thill, F. Mouchet, M. Carrière, L. Gauthier, W. Achouak, J. Rose, M. R. Wiesner and J.-Y. Bottero, in *Nanoethics and Nanotoxicology*, Springer, Editon edn., 2011, pp. 325-357.
8. ISO, *Nanotechnologies — Terminology and definitions for nano-objects — Nanoparticle, nanofibre and nanoplate*, 2008.
9. SCENIHR (Scientific Committee on Emerging and Newly Identified Health Risks), *Opinion on the scientific basis for the definition of the term “nanomaterial”*, 2010.
10. J. P. Holdren, C. R. Sunstein and I. A. Siddiqui, *Policy Principles for the U.S. Decision-making Concerning Regulation and Oversight of Applications of Nanotechnology and Nanomaterials*, Executive Office of the President, USA, USA, 2011.
11. A. D. Maynard, *Don't define nanomaterials*, *Nature*, 2011, **475**, 31-31.
12. EU, *Commission recommendation of 18 October 2011 on the definition of nanomaterial (2011/696/EU)*, *Official Journal L*, 2011, 38-40.
13. S. Foss Hansen, B. H. Larsen, S. I. Olsen and A. Baun, *Categorization framework to aid hazard identification of nanomaterials*, *Nanotoxicology*, 2007, **1**, 243 - 250.
14. Y. Ju-Nam and J. R. Lead, *Manufactured nanoparticles: An overview of their chemistry, interactions and potential environmental implications*, *Sci Total Environ*, 2008, **400**, 396-414.

15. B. Nowack, J. F. Ranville, S. Diamond, J. A. Gallego-Urrea, C. Metcalfe, J. Rose, N. Horne, A. A. Koelmans and S. J. Klaine, *Potential scenarios for nanomaterial release and subsequent alteration in the environment*, *Environ Toxicol Chem*, 2012, **31**, 50-59.
16. G. V. Lowry, K. B. Gregory, S. C. Apte and J. R. Lead, *Transformations of Nanomaterials in the Environment*, *Environmental Science & Technology*, 2012, 120601081904003.
17. R. Kaegi, A. Ulrich, B. Sinnet, R. Vonbank, A. Wichser, S. Zuleeg, H. Simmler, S. Brunner, H. Vonmont, M. Burkhardt and M. Boller, *Synthetic TiO<sub>2</sub> nanoparticle emission from exterior facades into the aquatic environment*, *Environ Pollut*, 2008, **156**, 233-239.
18. J. Farkas, H. Peter, P. Christian, J. A. Gallego Urrea, M. Hassellöv, J. Tuoriniemi, S. Gustafsson, E. Olsson, K. Hylland and K. V. Thomas, *Characterization of the effluent from a nanosilver producing washing machine*, *Environment International*, 2011, **37**, 1057-1062.
19. V. L. Colvin, *The potential environmental impact of engineered nanomaterials*, *Nat Biotechnol*, 2003, **21**, 1166-1170.
20. S. F. Hansen, A. Maynard, A. Baun and J. A. Tickner, *Late lessons from early warnings for nanotechnology*, *Nat. Nanotechnol.*, 2008, **3**, 444-447.
21. A. E. Nel, L. Mädler, D. Velegol, T. Xia, E. M. V. Hoek, P. Somasundaran, F. Klaessig, V. Castranova and M. Thompson, *Understanding biophysicochemical interactions at the nano-bio interface*, *Nature Materials*, 2009, **8**, 543-557.
22. M. Hasselov and F. von der Kammer, *Iron Oxides as Geochemical Nanovectors for Metal Transport in Soil-River Systems*, *Elements*, 2008, **4**, 401-406.
23. K. L. Plathe, F. von der Kammer, M. Hasselov, J. Moore, M. Murayama, T. Hofmann and M. F. Hochella, *Using FIFFF and aTEM to determine trace metal-nanoparticle associations in riverbed sediment*, *Environ. Chem.*, 2009, **7**, 82-93.
24. T. Hofmann and F. von der Kammer, *Estimating the relevance of engineered carbonaceous nanoparticle facilitated transport of hydrophobic organic contaminants in porous media*, *Environ Pollut*, 2009, **157**, 1117-1126.
25. J. Hammes, J. A. Gallego-Urrea and M. Hassellöv, *Geographically distributed classification of surface water chemical parameters influencing fate and behavior of nanoparticles and colloid facilitated contaminant transport*, *Water Research*, 2013, **47**.
26. A. D. Maynard, D. B. Warheit and M. A. Philbert, *The New Toxicology of Sophisticated Materials: Nanotoxicology and Beyond*, *Toxicol. Sci.*, 2010.
27. T. Xia, D. Malasarn, S. Lin, Z. Ji, H. Zhang, R. J. Miller, A. A. Keller, R. M. Nisbet, B. H. Harthorn, H. A. Godwin, H. S. Lenihan, R. Liu, J.

- Gardea-Torresdey, Y. Cohen, L. Mädler, P. A. Holden, J. I. Zink and A. E. Nel, *Implementation of a Multidisciplinary Approach to Solve Complex Nano EHS Problems by the UC Center for the Environmental Implications of Nanotechnology*, *Small*, 2012.
28. R. D. Handy, F. von der Kammer, J. R. Lead, M. Hasselov, R. Owen and M. Crane, *The ecotoxicology and chemistry of manufactured nanoparticles*, *Ecotoxicology*, 2008, **17**, 287-314.
29. R. Arvidsson, S. Molander, B. A. Sanden and M. Hasselov, *Challenges in Exposure Modeling of Nanoparticles in Aquatic Environments*, *Human and Ecological Risk Assessment*, 2011, **17**, 245-262.
30. P. Christian, F. Von der Kammer, M. Baalousha and T. Hofmann, *Nanoparticles: structure, properties, preparation and behaviour in environmental media*, *Ecotoxicology*, 2008, **17**, 326-343.
31. S. J. Klaine, P. J. J. Alvarez, G. E. Batley, T. F. Fernandes, R. D. Handy, D. Y. Lyon, S. Mahendra, M. J. McLaughlin and J. R. Lead, *Nanomaterials in the environment: Behavior, fate, bioavailability, and effects*, *Environ Toxicol Chem*, 2008, **27**, 1825-1851.
32. F. Gottschalk, R. W. Scholz and B. Nowack, *Probabilistic material flow modeling for assessing the environmental exposure to compounds: Methodology and an application to engineered nano-TiO<sub>2</sub> particles*, *Environ. Modell. Softw.*, 2010, **25**, 320-332.
33. F. Gottschalk, T. Sonderer, R. W. Scholz and B. Nowack, *Modeled Environmental Concentrations of Engineered Nanomaterials (TiO<sub>2</sub>, ZnO, Ag, CNT, Fullerenes) for Different Regions*, *Environmental Science & Technology*, 2009, **43**, 9216-9222.
34. N. Musee, M. Thwala and N. Nota, *The antibacterial effects of engineered nanomaterials: implications for wastewater treatment plants.*, *Journal of environmental monitoring : JEM*, 2011, **13**, 1164-1183.
35. A. Keller, S. McFerran, A. Lazareva and S. Suh, *Global life cycle releases of engineered nanomaterials*, *J. Nanopart. Res.*, 2013, **15**, 1-17.
36. F. Gottschalk, T. Sun and B. Nowack, *Environmental concentrations of engineered nanomaterials: Review of modeling and analytical studies*, *Environ Pollut*, 2013.
37. J. A. Gallego-Urrea, J. Tuoriniemi and M. Hasselov, *Applications of particle-tracking analysis to the determination of size distributions and concentrations of nanoparticles in environmental, biological and food samples*, *Trac-Trends Anal. Chem.*, 2011, **30**, 473-483.
38. N. T. Loux, Y. S. Su and S. M. Hassan, *Issues in Assessing Environmental Exposures to Manufactured Nanomaterials*, *International Journal of Environmental Research and Public Health*, 2011, **8**, 3562-3578.



39. R. Arvidsson, *Contributions to Emission, Exposure and Risk Assessment of Nanomaterials*, Chalmers University of Technology, 2012.
40. M. Elimelech, X. Jia, J. Gregory and R. Williams, *Particle Deposition & Aggregation: Measurement, Modelling and Simulation*, Butterworth-Heinemann, 1998.
41. M. Smoluchowski, *Versuch einer mathematischen Theorie der Koagulationskinetik kolloider Lösungen*, *Zeitschrift für Physikalische Chemie*, 1917, **92**, 129-168.
42. D. V. Chapman, *Water quality assessments: a guide to the use of biota, sediments and water in environmental monitoring*, E & Fm Spon London, 1996.
43. D. Zhou, A. I. Abdel-Fattah and A. A. Keller, *Clay particles destabilize engineered nanoparticles in aqueous environments*, *Environ Sci Technol*, 2012, **46**, 7520-7526.
44. J. T. K. Quik, I. Velzeboer, M. Wouterse, A. A. Koelmans and D. van de Meent, *Heteroaggregation and sedimentation rates for nanomaterials in natural waters*, *Water Research*, 2013.
45. K. A. Huynh, J. M. McCaffery and K. L. Chen, *Heteroaggregation of Multiwalled Carbon Nanotubes and Hematite Nanoparticles: Rates and Mechanisms*, *Environmental Science & Technology*, 2012, 120517094321003.
46. A. Praetorius, M. Scheringer and K. Hungerbühler, *Development of Environmental Fate Models for Engineered Nanoparticles—A Case Study of TiO<sub>2</sub> Nanoparticles in the Rhine River*, *Environmental Science & Technology*, 2012, **46**, 6705-6713.
47. J. A. Gallego-Urrea, J. Tuoriniemi, T. Pallander and M. Hasselov, *Measurements of nanoparticle number concentrations and size distributions in contrasting aquatic environments using nanoparticle tracking analysis*, *Environ. Chem.*, 2009, **7**, 67-81.
48. N. S. Wigginton, K. L. Haus and M. F. Hochella Jr, *Aquatic environmental nanoparticles*, *Journal of Environmental Monitoring*, 2007, **9**, 1306.
49. M. F. Hochella, D. Aruguete, B. Kim and A. S. Madden, eds. A. Brennan and W. H. Guo, Pan Stanford Publishing Pte. Ltd., Editon edn., 2012, vol. 8, pp. 978-981.
50. M. F. Hochella, S. K. Lower, P. A. Maurice, R. L. Penn, N. Sahai, D. L. Sparks and B. S. Twining, *Nanominerals, mineral nanoparticles, and earth systems*, *Science*, 2008, **319**, 631-635.
51. J. Buffle, K. J. Wilkinson, S. Stoll, M. Filella and J. Zhang, *A Generalized Description of Aquatic Colloidal Interactions: The Three-colloidal Component Approach*, *Environ. Sci. Technol.*, 1998, **32**, 2887-2899.

52. P. Biswas, W.-J. An and W.-N. Wang, eds. A. Brennan and W. H. Guo, Pan Stanford Publishing Pte. Ltd., Editon edn., 2012, vol. 8, pp. 978-981.
53. R. D. Handy, R. Owen and E. Valsami-Jones, *The ecotoxicology of nanoparticles and nanomaterials: current status, knowledge gaps, challenges, and future needs.*, *Ecotoxicology (London, England)*, 2008, **17**, 315-325.
54. P. Westerhoff and B. Nowack, *Searching for Global Descriptors of Engineered Nanomaterial Fate and Transport in the Environment*, *Accounts of chemical research*, 2012.
55. H. Zanker and A. Schierz, *Engineered nanoparticles and their identification among natural nanoparticles*, *Annual review of analytical chemistry*, 2012, **5**, 107-132.
56. J. Tuoriniemi, G. Cornelis and M. Hassellöv, *Size Discrimination and Detection Capabilities of Single-Particle ICPMS for Environmental Analysis of Silver Nanoparticles*, *Analytical Chemistry*, 2012, **84**, 3965-3972.
57. M. Hassellöv and R. Kaegi, in *Nanoscience and Nanotechnology: Environmental and human health implications*, eds. L. JR and S. E, Wiley Online Library, Editon edn., 2009, pp. 211-266.
58. S. Nangia and R. Sureshkumar, *Effects of nanoparticle charge and shape anisotropy on translocation through cell membranes*, *Langmuir*, 2012, **28**, 17666-17671.
59. M. Rycenga, C. M. Cobley, J. Zeng, W. Li, C. H. Moran, Q. Zhang, D. Qin and Y. Xia, *Controlling the Synthesis and Assembly of Silver Nanostructures for Plasmonic Applications*, *Chem. Rev.*, 2011, **111**, 3669-3712.
60. I. A. Khan, A. R. Afroz, J. R. Flora, P. A. Schierz, P. L. Ferguson, T. Sabo-Attwood and N. B. Saleh, *Chirality affects aggregation kinetics of single-walled carbon nanotubes*, *Environ Sci Technol*, 2013, **47**, 1844-1852.
61. H. G. Merkus, *Particle Size Measurements. Fundamentals, Practice, Quality*, Springer, 2009.
62. B. R. Jennings and K. Parslow, *Particle-Size Measurement - the Equivalent Spherical Diameter*, *P Roy Soc Lond a Mat*, 1988, **419**, 137-149.
63. J. S. Pedersen, *Analysis of small-angle scattering data from colloids and polymer solutions: modeling and least-squares fitting*, *Advances in Colloid and Interface Science*, 1997, **70**, 171-210.
64. P. C. Hiemenz and R. Rajagopalan, *Principles of colloid and surface chemistry*, Dekker, New York, 1997.
65. J. B. Falabella, T. J. Cho, D. C. Ripple, V. A. Hackley and M. J. Tarlov, *Characterization of Gold Nanoparticles Modified with Single-*

- Stranded DNA Using Analytical Ultracentrifugation and Dynamic Light Scattering*, *Langmuir*, 2010, **26**, 12740-12747.
66. J. Happel and H. Brenner, *Low Reynolds Number Hydrodynamics: With Special Applications to Particulate Media*, Prentice-Hall, 1983.
67. H. P. van Leeuwen, R. M. Town and J. Buffle, *Chemodynamics of soft nanoparticulate metal complexes in aqueous media: basic theory for spherical particles with homogeneous spatial distributions of sites and charges.*, *Langmuir : the ACS journal of surfaces and colloids*, 2011, **27**, 4514-4519.
68. M. Lattuada, H. Wu and M. Morbidelli, *Hydrodynamic radius of fractal clusters*, *J. Colloid Interface Sci.*, 2003, **268**, 96-105.
69. W. Pabst and E. Gregorova, *Characterization of particles and particle systems*, Institute of Chemical Technology Prague, Czech Republic, 2007.
70. L. M. Mosley, K. A. Hunter and W. A. Ducker, *Forces between Colloid Particles in Natural Waters*, *Environmental Science {&} Technology*, 2003, **37**, 3303-3308.
71. H. Greberg and R. Kjellander, *Charge inversion in electric double layers and effects of different sizes for counterions and coions*, *The Journal of Chemical Physics*, 1998, **108**, 2940-2953.
72. C. Labbez, B. Jönsson, M. Skarba and M. Borkovec, *Ion-Ion Correlation and Charge Reversal at Titrating Solid Interfaces*, *Langmuir*, 2009, **25**, 7209-7213.
73. T. L. Doane, C.-H. Chuang, R. J. Hill and C. Burda, *Nanoparticle  $\zeta$ -Potentials*, *Accounts of Chemical Research*, 2011, **45**, 317-326.
74. H. Ohshima, *A Simple Expression for Henry's Function for the Retardation Effect in Electrophoresis of Spherical Colloidal Particles*, *J. Colloid Interface Sci.*, 1994, **168**, 269-271.
75. K. Bourikas, T. Hiemstra and W. H. Van Riemsdijk, *Ion Pair Formation and Primary Charging Behavior of Titanium Oxide (Anatase and Rutile)*, *Langmuir*, 2001, **17**, 749-756.
76. J. Lyklema, *Overcharging, charge reversal: Chemistry or physics?*, *Colloids and Surfaces A: Physicochemical and Engineering Aspects*, 2006, **291**, 3-12.
77. G. Fritz, V. Schädler, N. Willenbacher and N. J. Wagner, *Electrosteric Stabilization of Colloidal Dispersions*, *Langmuir*, 2002, **18**, 6381-6390.
78. S. Lin and M. R. Wiesner, *Theoretical investigation on the interaction between a soft particle and a rigid surface*, *Chemical Engineering Journal*, 2012, **191**, 297-305.
79. S. Lin, Y. Cheng, J. Liu and M. R. Wiesner, *Polymeric Coatings on Silver Nanoparticles Hinder Autoaggregation but Enhance Attachment to Uncoated Surfaces*, *Langmuir*, 2012, **28**, 4178-4186.
80. J. Farkas, P. Christian, J. A. Gallego-Urrea, N. Roos, M. Hasselov, K. E. Tollefsen and K. V. Thomas, *Uptake and effects of manufactured*

- silver nanoparticles in rainbow trout (Oncorhynchus mykiss) gill cells, Aquat Toxicol*, 2011, **101**, 117-125.
81. J. Labille, J. Feng, C. Botta, D. Borschneck, M. Sammut, M. Cabie, M. Auffan, J. Rose and J.-Y. Bottero, *Aging of TiO<sub>2</sub> nanocomposites used in sunscreen. Dispersion and fate of the degradation products in aqueous environment, Environ Pollut*, 2010, **158**, 3482-3489.
82. R. Brown, *The miscellaneous botanical works of Robert Brown: Volume 1. (Edited by John J. Bennett)*. R. Hardwicke, London, 1866.
83. R. F. Rajter and R. H. French, *New perspectives on van der Waals–London interactions of materials. From planar interfaces to carbon nanotubes, Journal of Physics: Conference Series*, 2008, **94**, 012001.
84. J. N. Israelachvili, *Intermolecular and Surface Forces*, 3rd edn., Academic Press, Amsterdam, 2011.
85. V. A. Parsegian, *Van der Waals Forces: A Handbook for Biologists, Chemists, Engineers, and Physicists*, Cambridge University Press, 2005.
86. W. B. Russel, D. A. Saville and S. W., *Colloidal dispersions*, Cambridge, 1989.
87. H. Ohshima, *Biophysical chemistry of biointerfaces*, Wiley, Hoboken, NJ, USA, 2010.
88. R. Rajter, R. H. French, R. Podgornik, W. Y. Ching and V. A. Parsegian, *Spectral mixing formulations for van der Waals-London dispersion interactions between multicomponent carbon nanotubes, J Appl Phys*, 2008, **104**, 53513.
89. A. R. Petosa, D. P. Jaisi, I. R. Quevedo, M. Elimelech and N. Tufenkji, *Aggregation and Deposition of Engineered Nanomaterials in Aquatic Environments: Role of Physicochemical Interactions, Environmental Science & Technology*, 2010, null-null.
90. D. F. Evans and H. Wennerström, *The colloidal domain: where physics, chemistry, biology and technology meet*, 2nd edn., John Wiley and Sons, 1999.
91. T. Phenrat, J. E. Song, C. M. Cisneros, D. P. Schoenfelder, R. D. Tilton and G. V. Lowry, *Estimating Attachment of Nano- and Submicrometer-particles Coated with Organic Macromolecules in Porous Media: Development of an Empirical Model, Environmental Science & Technology*, 2010, **44**, 4531-4538.
92. M. Filella, *Freshwaters: which NOM matters?., Environ Chem Lett*, 2009, **7**, 21-35.
93. J. Buffle, K. J. Wilkinson, S. Stoll, M. Filella and J. Zhang, *A Generalized Description of Aquatic Colloidal Interactions: The Three-colloidal Component Approach, Environmental Science & Technology*, 1998, **32**, 2887-2899.

94. M. Filella and J. Buffle, *Factors controlling the stability of submicron colloids in natural-waters*, Symp on Colloids in the Aquatic Environment, London, England, 1992.
95. F. Loosli, P. Le Coustumer and S. Stoll, *TiO<sub>2</sub> nanoparticles aggregation and disaggregation in presence of alginate and Suwannee River humic acids. pH and concentration effects on nanoparticle stability*, *Water Res*, 2013, **47**, 6052-6063.
96. S. Diegoli, A. L. Manciuola, S. Begum, I. P. Jones, J. R. Lead and J. A. Preece, *Interaction between manufactured gold nanoparticles and naturally occurring organic macromolecules*, *Science of The Total Environment*, 2008, **402**, 51-61.
97. K. L. Chen, S. E. Mylon and M. Elimelech, *Enhanced aggregation of alginate-coated iron oxide (hematite) nanoparticles in the presence of calcium, strontium, and barium cations*, *Langmuir*, 2007, **23**, 5920-5928.
98. J. Liu, S. Legros, F. von der Kammer and T. Hofmann, *Natural organic matter concentration and hydrochemistry influence aggregation kinetics of functionalized engineered nanoparticles*, *Environ Sci Technol*, 2013, **47**, 4113-4120.
99. F. von der Kammer, S. Ottofuelling and T. Hofmann, *Assessment of the physico-chemical behavior of titanium dioxide nanoparticles in aquatic environments using multi-dimensional parameter testing*, *Environ Pollut*, 2010, **158**, 3472-3481.
100. K. L. Chen and M. Elimelech, *Interaction of Fullerene (C-60) Nanoparticles with Humic Acid and Alginate Coated Silica Surfaces: Measurements, Mechanisms, and Environmental Implications*, *Environmental Science & Technology*, 2008, **42**, 7607-7614.
101. D. Ramkrishna, in *Population Balances*, Academic Press, San Diego, Editon edn., 2000, pp. 117-195.
102. E. P. Honig, G. J. Roeberson and P. H. Wiersema, *Effect of hydrodynamic interaction on the coagulation rate of hydrophobic colloids*, *J. Colloid Interface Sci.*, 1971, **36**, 97-109.
103. M. Y. Lin, H. M. Lindsay, D. A. Weitz, R. C. Ball, R. Klein and P. Meakin, *Universality in colloid aggregation*, *Nature*, 1989, **339**, 360-362.
104. T. Abberger, in *Handbook of Powder Technology*, eds. M. J. H. A.D. Salman and J. P. K. Seville, Elsevier Science B.V., Editon edn., 2007, vol. Volume 11, pp. 1109-1186.
105. H.-C. Schwarzer and W. Peukert, *Prediction of aggregation kinetics based on surface properties of nanoparticles*, *Chemical Engineering Science*, 2005, **60**, 11-25.
106. C. N. Davies, *The Sedimentation and Diffusion of Small Particles*, *Proceedings of the Royal Society of London. Series A. Mathematical and Physical Sciences*, 1949, **200**, 100-113.

107. M. Mason and W. Weaver, *The Settling of Small Particles in a Fluid*, *Physical Review*, 1924, **23**, 412-426.
108. P. Hinderliter, K. Minard, G. Orr, W. Chrisler, B. Thrall, J. Pounds and J. Teegarden, *ISDD: A computational model of particle sedimentation, diffusion and target cell dosimetry for in vitro toxicity studies*, *Particle and Fibre Toxicology*, 2010, **7**, 36.
109. G. K. Batchelor, *Sedimentation in a dilute dispersion of spheres*, *Journal of Fluid Mechanics*, 1972, **52**, 245-268.
110. Clay Minerals Society and Organisation for Economic Co-operation Development, *Data Handbook for Clay Materials and Other Non-metallic Minerals: Providing Those Involved in Clay Research and Industrial Application with Sets of Authoritative Data Describing the Physical and Chemical Properties and Mineralogical Composition of the Available Reference Materials*, Pergamon Press, 1979.
111. L. Derrendinger and G. Sposito, *Flocculation Kinetics and Cluster Morphology in Illite/NaCl Suspensions*, *J. Colloid Interface Sci.*, 2000, **222**, 1-11.
112. S. K. Friedlander, *Smoke, dust and haze, fundamentals of aerosol behavior*, John Wiley & Sons, Inc., New York, 1977.
113. S. B. Grant, J. H. Kim and C. Poor, *Kinetic Theories for the Coagulation and Sedimentation of Particles*, *Journal of Colloid and Interface Science*, 2001, **238**, 238-250.
114. R. Salminen, M. J. Batista, M. Bidovec, A. Demetriades, B. De Vivo, W. De Vos, M. Duris, A. Gilucis, V. Gregorauskiene, J. Halamic, P. Heitzmann, A. Lima, G. Jordan, G. Klaver, P. Klein, J. Lis, J. Locutura, K. Marsina, A. Mazreku, P. J. O'Connor, S. Å. Olsson, R. T. Ottesen, V. Petersell, J. A. Plant, S. Reeder, I. Salpeteur, H. Sandström, U. Siewers, A. Steenfelt and T. Tarvainen, *FOREGS Geochemical Atlas of Europe, Part 1: Background Information, Methodology and Maps*, Geological Survey of Finland, Espoo, 2005.
115. European Environmental Agency, *WISE River basin districts (RBDs) - version 1.4 (06/2011)*, <http://www.eea.europa.eu/data-and-maps/data/wise-river-basin-districts-rbds-1>, Accessed 27th of June, 2012, 2012.
116. L. Brunet, D. Y. Lyon, E. M. Hotze, P. J. J. Alvarez and M. R. Wiesner, *Comparative Photoactivity and Antibacterial Properties of C60 Fullerenes and Titanium Dioxide Nanoparticles*, *Environmental Science & Technology*, 2009, **43**, 4355-4360.
117. M. Auffan, M. Pedeutour, J. Rose, A. Masion, F. Ziarelli, D. Borschneck, C. Chaneac, C. Botta, P. Chaurand, J. Labille and J. Y. Bottero, *Structural Degradation at the Surface of a TiO<sub>2</sub>-Based Nanomaterial Used in Cosmetics*, *Environ Sci Technol*, 2010, **44**, 2689-2694.

118. B. a. Miller-Chou and J. L. Koenig, *A review of polymer dissolution, Progress in Polymer Science*, 2003, **28**, 1223-1270.
119. P. Borm, *Research Strategies for Safety Evaluation of Nanomaterials, Part V: Role of Dissolution in Biological Fate and Effects of Nanoscale Particles, Toxicol Sci*, 2005, **90**, 23-32.
120. J. Y. Liu and R. H. Hurt, *Ion Release Kinetics and Particle Persistence in Aqueous Nano-Silver Colloids, Environ Sci Technol*, 2010, **44**, 2169-2175.
121. K. M. Metz, A. N. Mangham, M. J. Bierman, S. Jin, R. J. Hamers and J. A. Pedersen, *Engineered Nanomaterial Transformation under Oxidative Environmental Conditions: Development of an in vitro Biomimetic Assay, Environmental Science & Technology*, 2009, **43**, 1598-1604.
122. B. Kim, C. S. Park, M. Murayama and M. F. Hochella, *Discovery and Characterization of Silver Sulfide Nanoparticles in Final Sewage Sludge Products, Environmental Science & Technology*, 2010, **44**, 7509-7514.
123. R. Kaegi, A. Voegelin, B. Sinnet, S. Zuleeg, H. Hagendorfer, M. Burkhardt and H. Siegrist, *Behavior of Metallic Silver Nanoparticles in a Pilot Wastewater Treatment Plant, Environmental Science & Technology*, 2011, **45**, 3902-3908.
124. O. Choi, T. E. Clevenger, B. Deng, R. Y. Surampalli, L. Ross Jr and Z. Hu, *Role of sulfide and ligand strength in controlling nanosilver toxicity, Water Research*, 2009, **43**, 1879-1886.
125. V. Bansal, A. Ahmad and M. Sastry, *Fungus-mediated biotransformation of amorphous silica in rice husk to nanocrystalline silica, J Am Chem Soc*, 2006, **128**, 14059-14066.
126. T. Rohwerder, T. Gehrke, K. Kinzler and W. Sand, *Bioleaching review part A: progress in bioleaching: fundamentals and mechanisms of bacterial metal sulfide oxidation, Appl Microbiol Biot*, 2003, **63**, 239-248.
127. R. Kaegi, B. Sinnet, S. Zuleeg, H. Hagendorfer, E. Mueller, R. Vonbank, M. Boller and M. Burkhardt, *Release of silver nanoparticles from outdoor facades, Environmental Pollution*, 2010, **158**, 2900-2905.
128. R. Kaegi, A. Ulrich, B. Sinnet, R. Vonbank, A. Wichser, S. Zuleeg, H. Simmler, S. Brunner, H. Vonmont, M. Burkhardt and M. Boller, *Synthetic TiO<sub>2</sub> nanoparticle emission from exterior facades into the aquatic environment, Environ. Pollut.*, 2008, **156**, 233-239.
129. W. Wohlleben, S. Brill, M. W. Meier, M. Mertler, G. Cox, S. Hirth, B. v. Vacano, V. Strauss, S. Treumann, K. Wiench, L. Ma-Hock and R. Landsiedel, *On the Lifecycle of Nanocomposites: Comparing Released Fragments and their In-Vivo Hazards from Three Release Mechanisms and Four Nanocomposites, Small*, 2011, **7**, 2384-2395.

130. M. Baalousha, *Aggregation and disaggregation of iron oxide nanoparticles: Influence of particle concentration, pH and natural organic matter*, *Science of The Total Environment*, 2009, **407**, 2093-2101.
131. C. Levard, E. M. Hotze, B. P. Colman, A. L. Dale, L. Truong, X. Y. Yang, A. J. Bone, G. E. Brown, R. L. Tanguay, R. T. Di Giulio, E. S. Bernhardt, J. N. Meyer, M. R. Wiesner and G. V. Lowry, *Sulfidation of Silver Nanoparticles: Natural Antidote to Their Toxicity*, *Environmental Science & Technology*, 2013.
132. X. Liu, G. Chen, A. A. Keller and C. Su, *Effects of dominant material properties on the stability and transport of TiO<sub>2</sub> nanoparticles and carbon nanotubes in aquatic environments: from synthesis to fate*, *Environmental Science: Processes & Impacts*, 2013, **15**, 169-189.
133. D. E. Koppel, *Analysis of macromolecular polydispersity in intensity correlation spectroscopy - method of cumulants*, *Journal of Chemical Physics*, 1972, **57**, 4814-&.
134. H. Holthoff, S. U. Egelhaaf, M. Borkovec, P. Schurtenberger and H. Sticher, *Coagulation Rate Measurements of Colloidal Particles by Simultaneous Static and Dynamic Light Scattering*, *Langmuir*, 1996, **12**, 5541-5549.
135. A. Siripinyanond, S. Worapanyanond and J. Shiowatana, *Field-Flow Fractionation-Inductively Coupled Plasma Mass Spectrometry: An Alternative Approach to Investigate Metal-Humic Substances Interaction*, *Environmental Science & Technology*, 2005, **39**, 3295-3301.
136. T. Abe, S. Kobayashi and M. Kobayashi, *Aggregation of colloidal silica particles in the presence of fulvic acid, humic acid, or alginate: Effects of ionic composition*, *Colloids and Surfaces A: Physicochemical and Engineering Aspects*, 2011, **379**, 21-26.
137. S. Hillier, *Particulate composition and origin of suspended sediment in the R. Don, Aberdeenshire, UK*, *Science of The Total Environment*, 2001, **265**, 281-293.
138. V. Chanudet and M. Filella, *A Non-Perturbing Scheme for the Mineralogical Characterization and Quantification of Inorganic Colloids in Natural Waters*, *Environmental Science & Technology*, 2006, **40**, 5045-5051.